

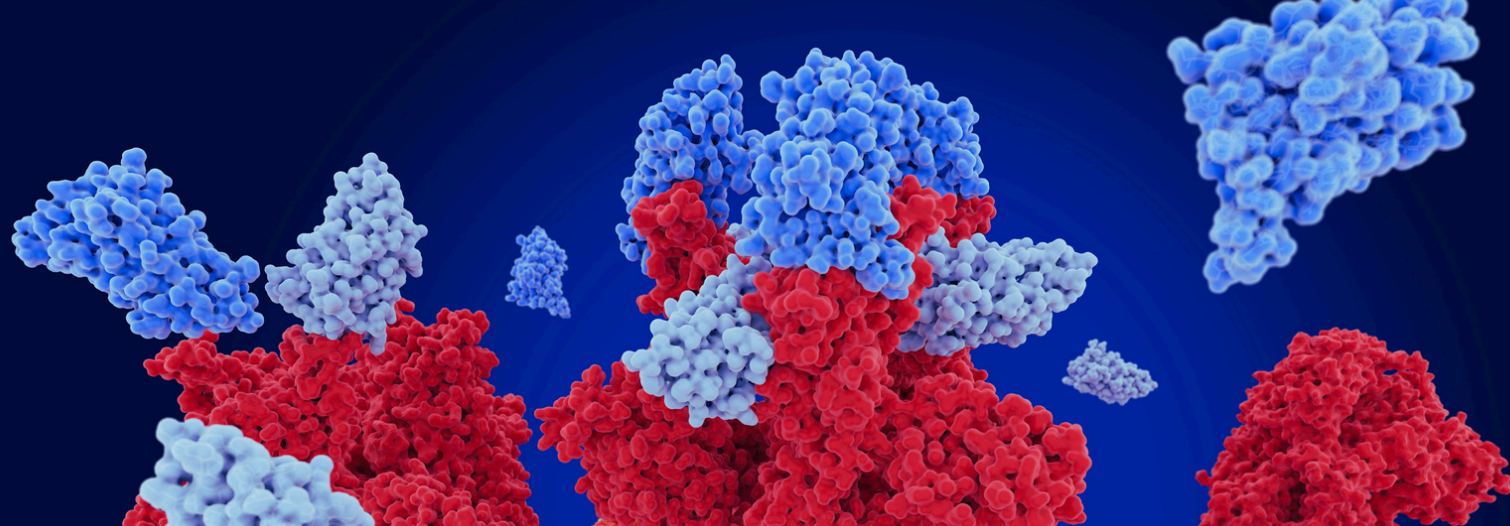
## VHH antibody engineering: a new tool for the therapeutic development pipeline



A FORTIS LIFE SCIENCES COMPANY



Taylor & Francis



## VHH antibody engineering: a new tool for the therapeutic development pipeline

# CONTENTS

- **Page 1 - Introduction**
- **Page 2 - Editorial:** IgG-VHH bispecific fusion antibodies: challenges and opportunities as therapeutic agents
- **Page 6 - Poster:** Nanomolar VHH binders of PD-L1 and other therapeutic targets from the AbNano™ VHH Naive Library
- **Page 7 - Research Article:** Chimeric antigens displaying GPR65 extracellular loops on a soluble scaffold enabled the discovery of antibodies, which recognized native receptor
- **Page 20 - Original Article:** Development and utilization of VHH antibodies derived from *Camelus Dromedarius* against foot-and-mouth disease virus
- **Page 26 - White Paper:** VHH antibodies: novel engineering strategies beget diverse applications



# Introduction

Antibody discovery is at the core of therapeutics research. However, despite their prevalence, antibodies' size and structure can impede their ability to specifically target certain epitopes.

VHH antibodies, also known as single-domain antibodies, are small antigen-binding fragments derived from camelid heavy-chain antibodies. Their small size and multispecific capabilities overcome many of the limitations of traditional antibodies, making them excellent candidates for drug discovery and development.

This eBook highlights how VHH antibodies are being developed and harnessed for therapeutic purposes, delving into the scaffolds used to generate and discover them and examples of their real-world applications against disease.



Beatrice Bowlby  
Digital Editor  
*BioTechniques*  
Beatrice.Bowlby@tandf.co.uk

## EDITORIAL



# IgG-VHH bispecific fusion antibodies: challenges and opportunities as therapeutic agents

Andreas V. Madsen <sup>a</sup>, Peter Kristensen <sup>b</sup> and Steffen Goletz <sup>a</sup><sup>a</sup>Department of Biotechnology and Biomedicine, Technical University of Denmark, Kgs. Lyngby, Denmark; <sup>b</sup>Department of Chemistry and Bioscience, Aalborg University, Aalborg, Denmark**ARTICLE HISTORY** Received 05 February 2024; Accepted 25 March 2024**KEYWORDS** IgG; VHH; IgG-VHH fusion; antibody; bispecific; bsAb; fusion protein

## 1. Introduction

Bispecific antibodies (bsAbs) have emerged as a promising class of therapeutic molecules, designed to simultaneously target two distinct antigens or epitopes. Simultaneous targeting of antigens permits synergistic functionalities beyond what can be obtained even with combinations of conventional monospecific antibodies [1]. A prime example is bispecific T-cell engagers that bridge tumor cells and T cells through binding of both a tumor associated antigen and CD3, thus targeting the T cells directly toward cells, expressing the tumor-associated antigen and mediating the CD8 T-cell killing of the tumor cells [2–4]. This work presents considerations on the formation of bsAbs through the fusion of antigen binding fragments from heavy-chain only antibodies (VHH) onto IgG scaffold to form bispecific IgG-VHH antibodies.

## 2. Characteristics of IgG-VHH fusions

BsAbs can be assembled in numerous different ways from various molecular building blocks to form a myriad of structurally diverse bsAb molecules, and the molecular configuration can be optimized to fit the therapeutic purpose [1]. Among these, IgG-VHH fusions, where small (~15 kDa) and monomeric VHH domains are fused onto IgG scaffolds, are a highly attractive way of forming stable and functional bsAbs [5]. The VHH molecules are the smallest naturally occurring antibody binding domains derived from heavy-chain only antibodies that can be found naturally in camelids and sharks. The VHH domains are monomeric and thus do not rely on pairing with a cognate light chain. This largely prevents chain mispairing and undesired self-association, which are common issues for scFv-IgG bsAbs that formed through the fusion of single-chain variable fragments (scFvs) onto IgG scaffolds [6]. Additionally, VHHs are known for their high stability and solubility, while generally being non-immunogenic, as they share high sequence identity with the human VH domains [7], which can be further improved through humanization campaigns.

The IgG-VHH fusions can be formed as both symmetric bsAbs, that adhere to the paired heavy chain–light chain symmetry of conventional monospecific antibodies (HC<sub>2</sub>LC<sub>2</sub>),

and as asymmetric bsAbs, e.g. by replacing one of the Fabs with a VHH domain [5,8]. Both types of bsAbs contain Fc domain that provides antibody effector functions through the binding of cognate Fcγ receptors as well as extended half-life through FcRn recycling and easy purification using Protein A. The construction of symmetric IgG-VHHs through simple the fusion of VHH domains is a reliable and conceptually easy way of forming bsAbs. The VHH can be fused to N- and/or C-termini of HC and/or LC, thus allowing flexibility with regard to valencies and molecular geometry. The HC<sub>2</sub>LC<sub>2</sub> symmetry is beneficial, because only two polypeptide chains need to be co-expressed, and therefore, the workflows closely resemble those of conventional monospecific antibodies which are established and very efficient. The recent exploration of a comprehensive panel of symmetric IgG-VHH bsAbs showed that fusion of VHH domains on IgG scaffolds is a robust way of forming functional and structurally diverse bsAbs with high thermodynamic stability and low aggregation propensity. Binding studies further confirmed that the IgG-VHH bsAbs were able to bind each target individually as well as simultaneously by being functionally bispecific [5]. The study also highlighted that the structural configuration influences the behavior of the molecules and that the molecular format is therefore a crucial factor to consider when developing IgG-VHH bsAbs. The molecular configuration of IgG-VHH bsAbs can be optimized to fit the therapeutic purpose, e.g. by tailoring the fusion site, the number of fused VHH domains (valency) as well as the spacing of antigen-binding domains by engineering the fusion site(s) and judicious linker design. It is also possible to form tandem VHH-Fc by replacing each Fab domain of the IgG with a tandem VHH to produce a tetravalent bsAb that does not contain any light chain. This construct requires expression of only a single polypeptide chain, thus greatly limiting the number of potential antibody-related impurities that can be formed from incomplete bsAb assembly. The simplicity of the tandem VHH-Fc construct makes it an attractive format that is currently being evaluated in a clinical setting (NCT03809624).

By replacing only a single Fab of the IgG with VHH or fusing the VHH on one of the HCs while also including mutations for

HC heterodimerization, such as knobs-into-holes [9], asymmetric IgG-VHH bsAbs can be constructed. These asymmetric bsAbs have the distinct advantage of containing only a single light chain which eliminates the risk of incorrect HC-LC pairing. The asymmetric nature of these IgG-VHH molecules allows full control of the valencies, and the bsAbs can also therefore be used for targets that require monovalent targeting of antigens where antigen crosslinking is highly undesired, such as CD3 [10]. The modular nature of VHH domains and IgG molecules allow very high flexibility with regard to fusion sites and the number of fused binding partners. This is not only applicable for tailoring the valencies of IgG-VHH but can also be used in the formation of tri- and tetraspecific antibodies [11].

While the fusion of VHH domains onto IgG scaffolds represents an attractive and robust means of forming bsAbs, it should be noted that the added complexity of molecules compared to the parent IgG risk introducing unexpected liabilities. This has been shown in a recent study where certain IgG-VHH configurations were found to be more aggregation prone than the parent IgG scaffold. This was particularly evident for two hexavalent bsAbs with VHH fused C-terminally on both HC and LC, suggesting that an added structural complexity of bsAbs can compromise colloidal stability [5]. Furthermore, the subclass of IgG scaffold should carefully be considered to match the intended IgG-VHH functionality [12].

### 3. Expert opinion

VHH domains are being increasingly recognized as attractive modular building blocks for constructing complex bsAbs with advanced functionalities. Despite their smaller size and relatively fewer complementarity-determining regions (CDRs), their binding affinities and versatilities are fully comparable to Fab and scFv. A recent comparison of a large number of paratope–epitope interfaces showed that VHH domains compensate for their smaller size by applying a larger proportion of both CDR and framework residues in the binding interface. This allows them to establish a similar number of total atom–atom contacts between the paratope and the epitope as conventional Fv antibodies, containing both VH and VL [13]. The efficient construction of IgG-VHH bsAbs can be broken down into the processes of (1) identifying suitable antigen-binding partners with the desired binding functionality and (2) judiciously combining the building blocks in an optimal molecular configuration that will allow the IgG-VHH to exert the desired biological function.

#### 3.1. Identifying molecular building blocks

VHs for therapeutic approaches can be obtained through the immunization of llamas in combination with the construction of large antibody libraries, such as phage or yeast display libraries, or via synthetic VHH antibody libraries with human or humanized frameworks [14]. As shown recently, VHH domains exhibit comparatively longer CDR3 than their Fv counterparts [13,15], thus making human VHH libraries with longer CDR3 desirable for therapeutic approaches which have been reported recently (Goletz, PEGS Europe, 2023). Since these processes to identify lead candidate VHH can be laborious and time consuming [12], computational tools are increasingly used to improve antibody

discovery campaigns. Examples include deep mining of antibody repertoires through next-generation sequencing coupled with advanced analytics [16] as well as modeling efforts to avoid selecting hits with liabilities that will negatively affect the developability profile and make them unsuitable as drug candidates [17]. The small and monomeric nature of VHH antibodies is also advantageous in these *in silico* workflows, because the lack of a VL partner makes uncertainties associated with proper VH-VL pairing obsolete. These uncertainties include reconstitution of native VH-VL pairs from individually sequenced genes or VH-VL packing during structural modeling.

#### 3.2. Assembling IgG-VHH bsAbs

After identifying an IgG scaffold and a suitable VHH domain to use as the exogenous fusion partner, the components must be combined to form the final IgG-VHH. The structural search space for IgG-VHs grows exponentially with linearly increasing number of parental antibodies, because the components can be combined in numerous different ways (Figure 1) [18]. Several parameters are important, such as fusion site, spatial orientation, valency, and linker lengths and design, which need to be carefully selected to achieve the desired biological activity and developability profile. While the optimal molecular configuration is likely to depend on target combinations and target availability, some trends were observed from a systematic study of a comprehensive panel of structurally diverse IgG-VHH bsAbs with mirrored specificities [5,8]. In these studies, the fusion of VHH to the HC in a symmetric format is favorable over fusion to LC. While all IgG-VHH bsAbs in the panel were functionally bispecific, i.e. able to bind both antigens individually and simultaneously, the molecular geometry showed influences on the binding affinity. The fusion of VHH to LC reduced the affinity of the scaffold Fv when linked N-terminally (3–10 fold affinity reduction), whereas fusion C-terminally on LC impaired the binding of VHH itself (4–5 fold affinity reduction). In contrast, VHH fusion to the HC showed much less pronounced effect on the binding affinity for both C- and N-terminally fused constructs. Since bsAbs often exhibit higher complexity than conventional IgGs, there is a need for assays that are capable of selectively characterizing the intricate binding functionality of bsAbs. Recently, an *in-solution* assay for dissecting bsAb binding functionality in complex dual binding environments without relying on potentially obstructive surface immobilization was introduced. The assay permits the assessment of simultaneous antigen binding through incremental increases in antibody–antigen complex sizes as well as determination of individual binding affinities even in higher order bsAb complexes, where more than one antigen is bound [8]. This *in-solution* assay based on flow-induced dispersion analysis also allows the determination of binding cooperativity and interference and can be applied even with complex sample matrices.

Another important aspect of bsAbs besides the direct targeting of the antigen and exerting the biological functionality is the developability profile, broadly referring to physicochemical properties that describes how likely it is a candidate can become an efficacious, safe, and manufacturable drug. Such important features include production yield, biophysical

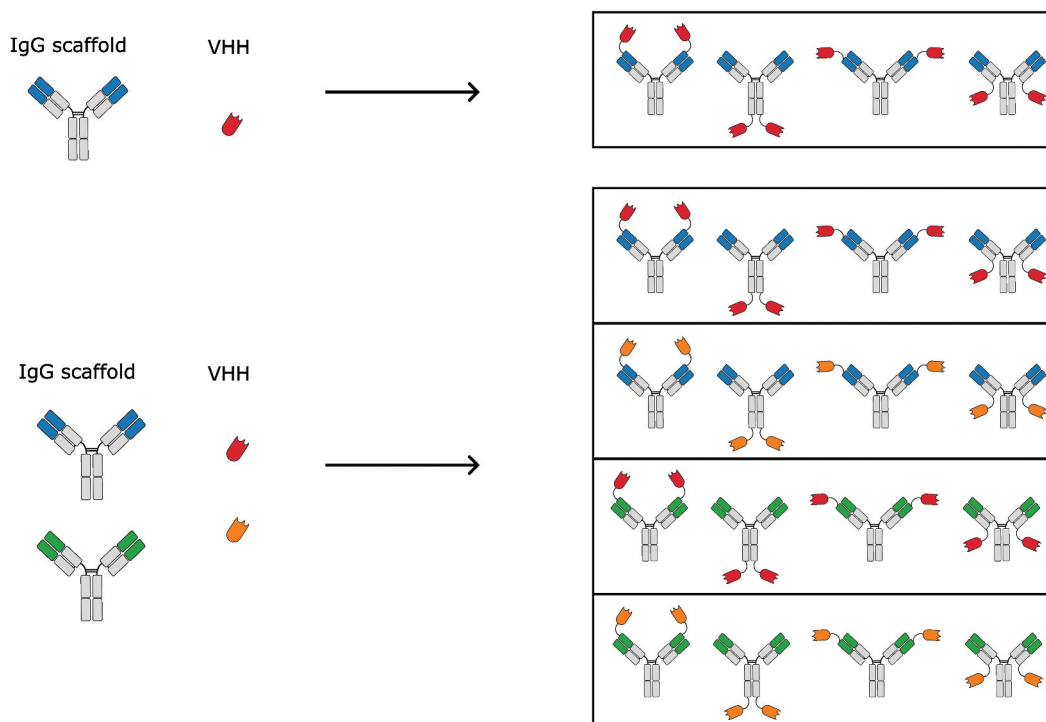


**Figure 1.** Combinatorial diversity of symmetric bsAb binder formats increases exponentially with increasing number of parental antibody building blocks. Only a selected set of symmetric tetraivalent bsAbs are shown, but the structural search space will become even bigger while also including asymmetric bsAbs or higher valency symmetric bsAbs.

stability, solubility, polyreactivity and immunogenicity. The bispecific IgG-VHH format can be seen as favorable in respect to biophysical stability and yield. The thermal stabilities of the symmetric IgG-VHH bsAb panel were generally high, and aggregation propensities were low, both comparable to IgG1 molecules [5]. Asymmetric formats using VHH as fusion partner are also seen to be robust in respect to the VHH part, while the thermal stability is somewhat reduced compared to IgG1 and symmetric formats [7], since most platforms for HC heterodimerization of asymmetric bsAbs are based on CH3 engineering known to negatively affect thermal stability. In respect to manufacturability, all the IgG-VHH bsAbs with VHH fused on HC fusion of VHH to HC showed an increase in productivity compared to the parent IgG1, while fusion of VHH to LC appeared less favorable [5]. Downstream workflows can make efficient use of Protein A purification and closely resemble those of conventional IgG1 for symmetric IgG-VHH. Most research on antibody developability has been conducted with conventional monospecific IgG molecules, and there is thus a need for a more systematic evaluation of developability liabilities for bsAbs such as IgG-VHH.

#### 4. Conclusion

Conclusively, IgG-VHH bsAbs present as attractive therapeutic agents that can be robustly assembled with high versatility to fit the intended mechanism of action. The small and monomeric nature of VHH domains make them highly suitable as exogenous fusion partners that bypass many of the issues often encountered for scFvs, containing both VH and VL. While the

ability to assemble IgG-VHH bsAbs with diverse molecular geometries allows for tailoring the bsAb to fit the therapeutic need, it also creates a large structural search space. The molecular configuration has a profound impact on the activity and behavior of the bsAbs. Recently described patterns for preferable fusion sites and geometries can help effectively exploring the search space to identify optimal bsAb binder formats and to generate optimized bispecific therapeutic candidates.

#### Funding

This work was supported by The Novo Nordisk Foundation Grant NNF19SA0056783, NNF19SA0057794, and NNF20SA0066621.

#### Declaration of interest

The authors have no relevant affiliations or financial involvement with any organization or entity with a financial interest in or financial conflict with the subject matter or materials discussed in the manuscript. This includes employment, consultancies, honoraria, stock ownership or options, expert testimony, grants or patents received or pending, or royalties.

#### Reviewer disclosures

Peer reviewers on this manuscript have no relevant financial or other relationships to disclose.

#### ORCID

Andreas V. Madsen  <http://orcid.org/0000-0002-8449-9691>  
 Peter Kristensen  <http://orcid.org/0000-0001-7205-6853>  
 Steffen Goletz  <http://orcid.org/0000-0003-1463-5448>

## References

1. Labrijn AF, Janmaat ML, Reichert JM, et al. Bispecific antibodies: a mechanistic review of the pipeline. *Nat Rev Drug Discov.* 2019;18(8):585–608. doi: [10.1038/s41573-019-0028-1](https://doi.org/10.1038/s41573-019-0028-1)
2. Hoffmann P, Hofmeister R, Brischwein K, et al. Serial killing of tumor cells by cytotoxic T cells redirected with a CD19-/CD3-bispecific single-chain antibody construct. *Int J Cancer.* 2005;115:98–104. doi: [10.1002/ijc.20908](https://doi.org/10.1002/ijc.20908)
3. Löffler A, Kufer P, Lutterbüse R, et al. A recombinant bispecific single-chain antibody, CD19 × CD3, induces rapid and high lymphoma-directed cytotoxicity by unstimulated T lymphocytes. *Blood.* 2000;95:2098–2103. doi: [10.1182/blood.V95.6.2098](https://doi.org/10.1182/blood.V95.6.2098)
4. Seckinger A, Majocchi S, Moine V, et al. Development and characterization of NILK-2301, a novel CEACAM5×CD3 κλ bispecific antibody for immunotherapy of CEACAM5-expressing cancers. *J Hematol Oncol.* 2023;16(1):117. doi: [10.1186/s13045-023-01516-3](https://doi.org/10.1186/s13045-023-01516-3)
5. Madsen AV, Kristensen P, Buell AK, et al. Generation of robust bispecific antibodies through fusion of single-domain antibodies on IgG scaffolds: a comprehensive comparison of formats. *MAbs.* 2023;15(1):2189432. doi: [10.1080/19420862.2023.2189432](https://doi.org/10.1080/19420862.2023.2189432)
6. Cao M, Wang C, Chung WK, et al. Characterization and analysis of scFv-IgG bispecific antibody size variants. *MAbs.* 2018;10(8):1236–1247. doi: [10.1080/19420862.2018.1505398](https://doi.org/10.1080/19420862.2018.1505398)
7. Muyldermans S. Nanobodies: natural single-domain antibodies. Kornberg R, editor. *Annu Rev Biochem.* 2013;82:775–797. doi: [10.1146/annurev-biochem-063011-092449](https://doi.org/10.1146/annurev-biochem-063011-092449)
8. Madsen AV, Mejias-Gomez O, Pedersen LE, et al. Immobilization-free binding and affinity characterization of higher order bispecific antibody complexes using size-based microfluidics. *Anal Chem.* 2022;94(40):13652–13658. doi: [10.1021/acs.analchem.2c02705](https://doi.org/10.1021/acs.analchem.2c02705)
9. Atwell S, Ridgway JBB, Wells JA, et al. Stable heterodimers from remodeling the domain interface of a homodimer using a phage display library. *J Mol Biol.* 1997;270(1):26–35. doi: [10.1006/jmbi.1997.1116](https://doi.org/10.1006/jmbi.1997.1116)
10. Lee HY, Contreras E, Register AC, et al. Development of a bioassay to detect T-cell-activating impurities for T-cell-dependent bispecific antibodies. *Sci Rep.* 2019;9(1):3900. doi: [10.1038/s41598-019-40689-1](https://doi.org/10.1038/s41598-019-40689-1)
11. Yanakieva D, Pekar L, Evers A, et al. Beyond bispecificity: controlled fab arm exchange for the generation of antibodies with multiple specificities. *MAbs.* 2022;14(1):2018960. doi: [10.1080/19420862.2021.2018960](https://doi.org/10.1080/19420862.2021.2018960)
12. Yu J, Song Y, Tian W. How to select IgG subclasses in developing anti-tumor therapeutic antibodies. *J Hematol Oncol.* 2020;13(1):45. doi: [10.1186/s13045-020-00876-4](https://doi.org/10.1186/s13045-020-00876-4)
13. Madsen AV, Mejias-Gomez O, Pedersen LE, et al. Structural trends in antibody-antigen binding interfaces: a computational analysis of 1833 experimentally determined 3D structures. *Computat Struct Biotechnol J.* 2024;23:199–211. doi: [10.1016/j.csbj.2023.11.056](https://doi.org/10.1016/j.csbj.2023.11.056)
14. Mandrup OA, Friis NA, Lykkemark S, et al. A novel heavy domain antibody library with functionally optimized complementarity determining regions. *PLoS One.* 2013;8(10):e76834. doi: [10.1371/journal.pone.0076834](https://doi.org/10.1371/journal.pone.0076834)
15. Mejias-Gomez O, Madsen AV, Skovgaard K, et al. A window into the human immune system: comprehensive characterization of the complexity of antibody complementary-determining regions in functional antibodies. *MAbs.* 2023;15(1):2268255. doi: [10.1080/19420862.2023.2268255](https://doi.org/10.1080/19420862.2023.2268255)
16. Greiff V, Miho E, Menzel U, et al. Bioinformatic and statistical analysis of adaptive immune repertoires. *Trends Immunol.* 2015;36(11):738–749. doi: [10.1016/j.it.2015.09.006](https://doi.org/10.1016/j.it.2015.09.006)
17. Raybould MIJ, Marks C, Krawczyk K, et al. Five computational developability guidelines for therapeutic antibody profiling. *Proceedings of the National Academy of Sciences of the United States of America.* 2019;116:p. 4025–4030.
18. Dengl S, Mayer K, Bormann F, et al. Format chain exchange (FORCE) for high-throughput generation of bispecific antibodies in combinatorial binder-format matrices. *Nat Commun.* 2020;11(1):4974. doi: [10.1038/s41467-020-18477-7](https://doi.org/10.1038/s41467-020-18477-7)

Qiang Chen, Fiona H.Y. Yuen, Monique N. Navarro, Kallie Kilchrist, and Sam Sugerman

Department of VHH Discovery, Abcore®, a Fortis Life Sciences® company. Correspondence to ssugerman@fortislife.com

## Background

VHH domains, derived from the variable heavy chain of the heavy-chain-only IgG2 and IgG3 domains in camelids, represent a small, single-domain antibody fragment. VHH domains have been successfully applied to technologies such as bispecific therapeutic molecules.

Discovering novel VHH domains can take place by multiple workflows, including using B-cell sorting and using display libraries. Within display libraries, the library is generally one of three classes of molecule: synthetic molecules, immunederived molecules, or naïve germline molecules. Each approach has its own unique advantages and applications.

Here, we present the construction and early validation of a large naïve library from llamas and alpacas. The data suggests that this library, the AbNano™ VHH Naive Library, may be well-suited for rapid discovery of VHH domains binding to therapeutic targets with varying levels of affinity.

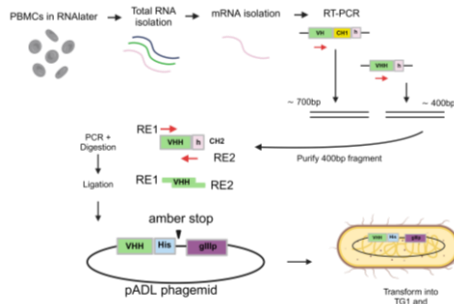


Figure 1: Overview of the library construction process. A total of  $1.12 \times 10^{10}$  transformants were collected from 13 sublibraries.

## Library Construction

The library was constructed from 103 naïve animals: 77 llamas and 26 alpacas. A total of  $1.51 \times 10^{10}$  PBMC cells were collected and used for library construction.

Libraries were constructed using species-specific primers. A total of 13 sublibraries were constructed through transformation. The total number of transformants for the library was  $1.12 \times 10^{10}$  cfu. Transformants were analyzed by Sanger and the individual sublibraries were analyzed by next generation sequencing at a total read count of 1.71 M reads using GeneWiz® Amplicon-EZ services from Azena Life Sciences. NGS reads from each sublibrary were combined and analyzed using Geneious Biologics.

The theoretical diversity of this library is difficult to predict due to variations in VHH-presenting heavy-chain-only IgG ratios among PBMCs, but sequencing data suggests that this library is transformation-limited in its diversity. Minimal redundancy was measured, and the library is generally free from bias or other cloning artifacts in its construction. Based on the unique cluster frequency, the in-frame VHH rate, and the number of representative transformants, we estimate the maximum possible library size of the naïve VHH library to be  $6.48 \times 10^9$  unique clonal VHH.

Library bacterial stocks were grown to log phase, infected by M13KO7, PEG precipitated, and the pooled phage was titered. Phage were normalized in PBS + 20% glycerol and aliquoted as 1 mL tubes frozen and stored at  $-80^\circ\text{C}$ .

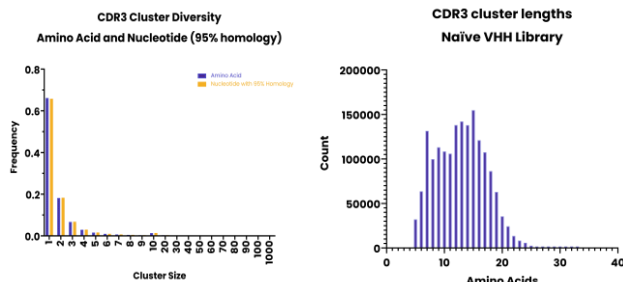


Figure 2: Comparison of cluster diversity for amino acid identity of CDR3 and for 95% homologous nucleotide identity of CDR3 suggests that there is minimal inherent bias in the final constructed library independently of any call or mutation artifacts.

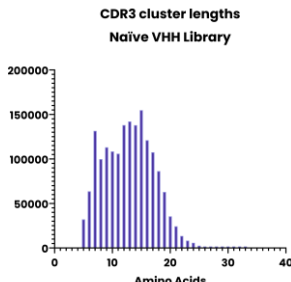


Figure 3: Histogram of length distribution in CDR3 of the VHH domains in the library. CDR3 length distribution of the pooled naïve library fits well with existing literature values for naïve camelid CDR3 and has good representation of CDR3 lengths from 5-22 residues in length.

## Panning and Screening

Phage selections were performed from the pooled phage input. Round 1 panning was performed with approximately  $2.5 \times 10^{10}$  pfu of phage. Here, we present campaigns against three separate targets of interest: INSR ECD, EGFR ECD, and PD-L1 ECD. All antigens were purchased commercially from Acro Biosystems.

For INSR $\beta$  panning, the recombinant antigen (residues H28-K944 of accession number P06213-2 with a C-terminal His tag) was adsorbed onto polystyrene plates. Phage was eluted by triethylamine after panning and PEG-precipitated between rounds. Clonal shockate screening generated 47 hits above the threshold of  $A_{405} > 0.4$ , with 29 unique binders by CDR3 analysis. Clone AbN3c-F01 (531 nM  $EC_{50}$ , Figure 5) was the most abundant clone in the sequenced pool.

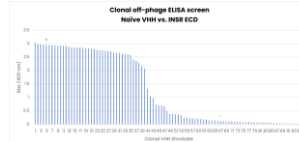


Figure 4. Clonal crude VHH were prepared by osmotic shock and assayed against recombinant INSR adsorbed on polystyrene plates. The single-point binding was detected by HRP-anti-VHH conjugate and ABTS.

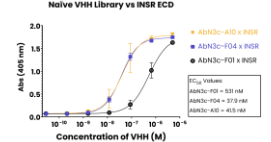


Figure 5. INSR lead VHH identified from clonal screen data were purified by Ni-NTA and assayed in duplicate titration. Binding was visualized with HRP-anti-VHH conjugate and ABTS.

Recombinant human epidermal growth factor (residues A310-C620 of accession number P00533-1 with C-terminal biotinylated Avi tag and poly-His) was pre-bound to streptavidin-coated magnetic beads. Phage was eluted by triethylamine after panning, and unprecipitated supernatant was used for further rounds. Clonal shockate screening generated 34 hits above the threshold of  $A_{405} > 0.4$ , but only 7 unique sequences by CDR3 analysis. AbN16-E07 was a dominant clonotype comprising 14 of the 34 hits.

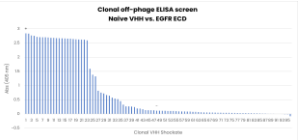


Figure 6. Clonal crude VHH were prepared by osmotic shock and assayed against recombinant EGFR bound to streptavidin plates. The single-point binding was detected by HRP-anti-VHH conjugate and ABTS.

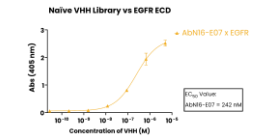


Figure 7. EGFR lead VHH AbN16-E07 identified from clonal screen data were purified by Ni-NTA, then assayed in duplicate titration. Binding was visualized with HRP-anti-VHH conjugate and ABTS.

Recombinant human PD-L1 (residues F19-Y134 from accession number Q9NZQ7-1 with C-terminal biotinylated Avi tag and poly-His) was incubated with blocked phage before being pulled down by addition of streptavidin-coated magnetic beads. Phage was eluted by triethylamine after panning and PEG-precipitated between rounds. 470 clones were screened by single point ELISA, generating 147 hits above the threshold of  $A_{405} > 0.4$  with 68 unique sequences identified from the 470 clones screened. This represents a unique hit rate of 14.5%.

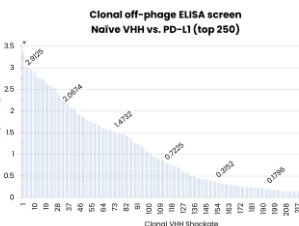


Figure 8. Clonal crude VHH were prepared by osmotic shock and assayed against recombinant PD-L1 bound to streptavidin plates. The single-point binding was detected by HRP-anti-VHH conjugate and ABTS.

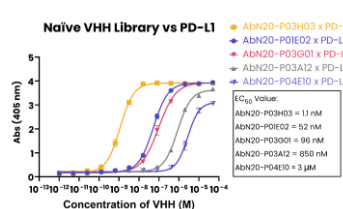


Figure 9. Five clones with varying single-point ELISA signal (P03H03 = 3.38, P01E02 = 3.00, P03G01 = 2.91, P03A12 = 0.62, P04E10 = 1.23) were purified by Ni-NTA then assayed in duplicate titration. Binding was visualized with HRP-anti-VHH conjugate and ABTS.

## Conclusions & Future Directions

Early validation of the AbNano™ VHH Naive Library suggests that the library is diverse and well-suited for rapid discovery of VHH domains binding to protein targets in a range of panning conditions. There is evidence to suggest that PEG precipitation between rounds minimizes the clonotype collapse at round 3. There is evidence to suggest that clones with approximately three orders of magnitude difference in affinity can be recovered side-by-side.

Future directions with this library are abundant. Additional panning verification datasets will yield greater confidence in library quality, especially against atypical antigens or antigen presentations. Semi-synthetic methods to diversify the library pool may be appealing at first, but due to the fully natural framework sampling such methods would inadvertently reduce the diversity in the frameworks. Individual hit and lead molecules are appealing to characterize and develop. Lead molecules derived from this library may also be independently engineered toward therapeutic applications.


## Acknowledgements

The authors wish to thank JJ and DB for helpful comments and assistance in the early conception and facilitation of this work, BM and AMW for their work at launch, and the entire Abcore team for their work on this project from conception to characterization.

GeneWiz® and Azena are trademarks of Azena Life Sciences  
ACROBiosystems is a trademark of ACROBiosystems Inc.  
Geneious is a trademark of Biomatters Inc.  
Image 1 was created with BioRender.com.  
GraphPad Prism® is a registered trademark of GraphPad Software, LLC. Images 2-9 were created in GraphPad Prism.



## Chimeric antigens displaying GPR65 extracellular loops on a soluble scaffold enabled the discovery of antibodies, which recognized native receptor

Janine Barrett <sup>a,b</sup>, Seppe Leysen<sup>a</sup>, Cécile Galmiche<sup>a</sup>, Hussein Al-Mossawi<sup>b</sup>, Paul Bowness<sup>b</sup>, Thomas E. Edwards<sup>c</sup>, and Alastair D.G. Lawson<sup>a</sup>

<sup>a</sup>UK Research Department, UCB Pharma, Slough, UK; <sup>b</sup>Nuffield Department of Orthopaedics, Rheumatology and Musculoskeletal Sciences, University of Oxford, Oxford, UK; <sup>c</sup>US Research Department, UCB Pharma, Bainbridge Island, WA, USA

### ABSTRACT

GPR65 is a proton-sensing G-protein coupled receptor associated with multiple immune-mediated inflammatory diseases, whose function is relatively poorly understood. With few reagents commercially available to probe the biology of receptor, generation of an anti-GPR65 monoclonal antibody was desired. Using soluble chimeric scaffolds, such as ApoE3, displaying the extracellular loops of GPR65, together with established phage display technology, native GPR65 loop-specific antibodies were identified. Phage-derived loop-binding antibodies recognized the wild-type native receptor to which they had not previously been exposed, generating confidence in the use of chimeric soluble proteins to act as efficient surrogates for membrane protein extracellular loop antigens. This technique provides promise for the rational design of chimeric antigens in facilitating the discovery of specific antibodies to GPCRs.

### Research Highlights

- This technique offers a viable approach for antibody discovery to difficult GPCRs.
- Structurally relevant, soluble chimeric scaffold proteins of GPR65 were generated.
- Chimeric antigens were used to identify GPR65-specific antibodies by phage display.

### ARTICLE HISTORY

Received 26 September 2023  
Revised 20 December 2023  
Accepted 21 December 2023

### KEYWORDS

GPCR; GPR65; phage display; chimeric protein antigens; monoclonal antibody generation

## Introduction


Ankylosing spondylitis (AS) is the prototypical seronegative spondyloarthritis, presenting with chronic inflammation primarily in the spine and sacroiliac joints, often in association with extra-articular features and comorbidities including inflammatory bowel disease and psoriasis [1,2]. While current therapeutic strategies for AS include the use of biologics to neutralize specific proinflammatory cytokines, many patients exhibit an inadequate clinical response to last-line therapies [3,4]. With significant unmet medical need, further research is required to fully understand the pathogenesis of this disease and elucidating the pathogenic role of genetically associated proteins will be key in developing effective therapeutics.

Genome wide association studies have identified GPR65 association with many immune-mediated diseases, including AS [5,6]; however, its pathogenic role remains unknown.

Discovered in 1996, GPR65 is a proton-sensing G protein coupled receptor (GPCR) family member, which becomes optimally activated at pH 6.4–6.8, leading to G<sub>s</sub> protein signaling and resulting in the accumulation of intracellular cAMP (cyclic adenosine monophosphate) [7,8]. GPR65 mRNA is predominantly expressed in the spleen, thymus, and peripheral blood leucocytes [9], therefore, the receptor is hypothesized to play an important role in the immune system.

GPCRs are highly conserved cell surface receptors which transduce extracellular signals into physiological effects and represent the largest family of proteins encoded by the human genome. Through their involvement in many key processes, their dysfunction contributes to many human diseases. Historically, there has been intense interest in the expansive GPCR family, and they still stand as the

**CONTACT** Janine Barrett  [janine.murray@UCB.com](mailto:janine.murray@UCB.com)  US Research Department, UCB Pharma, 208 Bath Road, Slough, Berkshire SL1 3WE, UK

 Supplemental data for this article can be accessed online at <https://doi.org/10.1080/21655979.2023.2299522>

© 2024 The Author(s). Published by Informa UK Limited, trading as Taylor & Francis Group. This is an Open Access article distributed under the terms of the Creative Commons Attribution License (<http://creativecommons.org/licenses/by/4.0/>), which permits unrestricted use, distribution, and reproduction in any medium, provided the original work is properly cited. The terms on which this article has been published allow the posting of the Accepted Manuscript in a repository by the author(s) or with their consent.

largest group of therapeutic targets, with most successful approaches targeting GPCRs with small molecules and peptides [10]. Despite decades of work, there are still only two approved GPCR targeted therapeutic antibodies, speaking to the technical challenges associated with identifying functional antibodies against GPCRs, and the need to advance extracellular loop display [11]. The creation of soluble antigens designed from the extracellular domains of calcitonin gene-related peptide linked to Fc domains enabled the discovery of erenumab, the first FDA approved antibody against a GPCR [12]. Alternatively, mogamulizumab was generated through the humanization of a chimeric mouse anti-CCR4 antibody, raised by immunizing a mouse with a peptide consisting of only 27 amino acids from human CCR4 [13,14].

Here, we use rationally designed chimeric protein scaffolds based on human apolipoprotein E3 (ApoE3) to present extracellular loops (ECL) of a GPCR as antigens in phage display, to discover GPR65-specific antibodies capable of recognizing native cell-expressed protein.

## Results

Work carried out in the vaccine field suggested that substituting structures of interest onto protein scaffolds, termed ‘epitope transplantation,’ can elicit an immune response to the antigen [15]. Within the seven-transmembrane structure of GPR65, the extracellular loops would likely exit from and enter back into alpha helices. Hence, three constructs were designed to utilize the 4 alpha-helix bundle structure of soluble ApoE3, with each of the preserved GPR65 ECL substituted for the wild type (WT) residues 105–109 (‘LGQST’) of ApoE3; in turn mimicking the membrane protein ECL leaving and entering a helix on each side (Figure 1a).

Additional constructs were also designed to incorporate several amino acids of the helices that lead into and away from the loop from the GPR65 sequence, to see if a more representative reflection of the backbone would provide a closer structure of the loops within the native protein. Limits of these alterations along the two helices were calculated upon the identification of

a seemingly critical interaction (Figure 1a, represented as red residues), required to maintain structural integrity of the protein. Finally, an additional His-Avi-TEV site was included within the construct design to aid purification of the protein, as well as biotinylation for downstream use.

Analysis of cell lysates, before and after induction, verified the expression of the chimeric proteins from bacteria. Next, the solubility of the chimeric proteins was assessed by separating the cell lysate (after induction) into a soluble and insoluble fraction through centrifugation. Majority of the proteins contained sequence changes that were well tolerated and found in the soluble fraction, whilst those where amino acids of the backbones were replaced with GPR65 residues (represented by +2aa, +4aa and +6aa), remained in the insoluble fraction (Figure 1b).

The chimeric proteins with direct loop substitutes went on to be used as antigens within a phage display campaign (Figure 2a) to pan 3 established UCB phage libraries. Two libraries of naïve human single chain variable fragments (scFv), each created independently from different donors, and a library of llama variable domain of heavy chain only antibodies (VHH) were included to increase diversity, aiming to expose the small (<30 amino acid) GPR65 ECL epitopes to advantageous antibody formats and diversity.

As peptides were acting as the antigen, the panning strategy was designed to increase efficiency by pooling all three constructs, each representing one of the GPR65 ECL, as well as maintaining a high concentration throughout the three panning rounds. Importantly, the epitopes of interest presented by the chimeric constructs were a small portion of the whole protein, therefore throughout the later panning rounds, subtraction pans were also incorporated. WT ApoE3 (Figure 2a, yellow boxes) was used to remove backbone binders and encourage only those recognizing the substituted loops of interest to become enriched.

Once panning was complete, monoclonal antibodies were rescued, and antibody-containing supernatant were screened by ELISA, identifying 163 antigen-specific binders (Figure 2b). Of the antibodies derived from the VHH library, the subtraction pan did not appear to enrich loop-specific binders, resulting in more from those not exposed to WT ApoE3. The scFv libraries

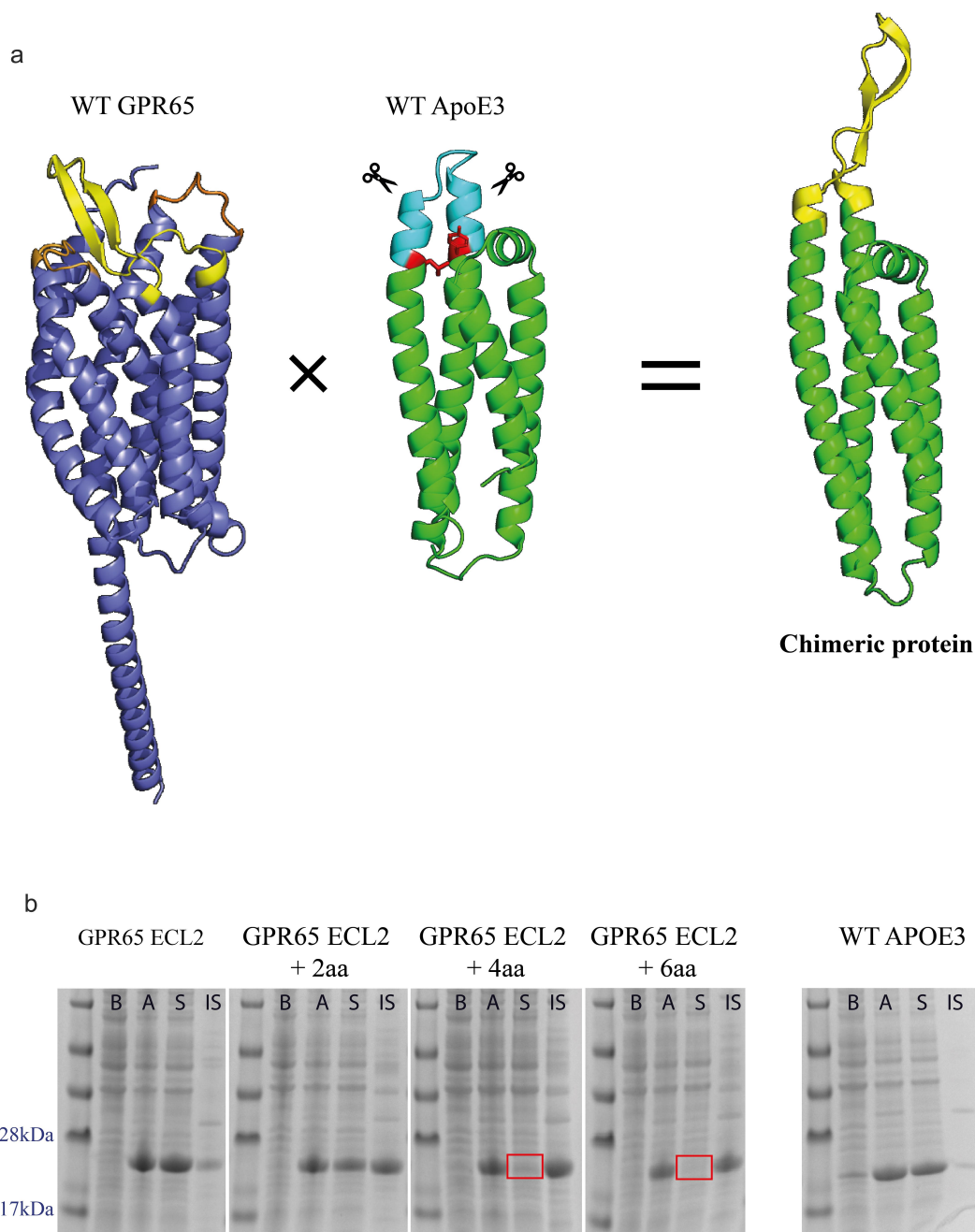


**Figure 1.** Expression of GPR65 chimeric constructs as soluble proteins. a) AlphaFold models representing human GPR65 (Uniprot entry Q8IYL9), truncated human apolipoprotein E (Uniprot entry P02649, PDB 1BZ4) and a representative example of the chimeric proteins, here displaying ECL2 of GPR65 (yellow) from the ApoE3 backbone (green). The transmembrane and ICL of GPR65 are in dark blue, with alternative GPR65 ECL in orange. Within the WT ApoE3 protein, the light blue region indicates the substituted residues, with red sites representing critical interactions between the two helices, which maintain structural integrity of the protein. b) SDS-PAGE gel of cell lysates before (b) and after (a) induction, and soluble (S) and insoluble (IS) fractions of expressed proteins for chimeric constructs with ECL2, representative for both ECL1 and ECL3. The + 'x'aa represents how many amino acids on each side of the loop, as part of the helix, were also substituted with those from native GPR65. Correct bands are observed between 22 and 23kDa. Red squares represent a lack of soluble protein.

led to a higher hit rate of antigen-specific antibodies; with enrichment of loop-specific antibodies through the inclusion of a subtraction step (at either rounds 2 or 3) and resulted in fewer

ApoE3 backbone binders. The additional panning round for scFv libraries over the VHH library was due to library size differences (Figure 2b).

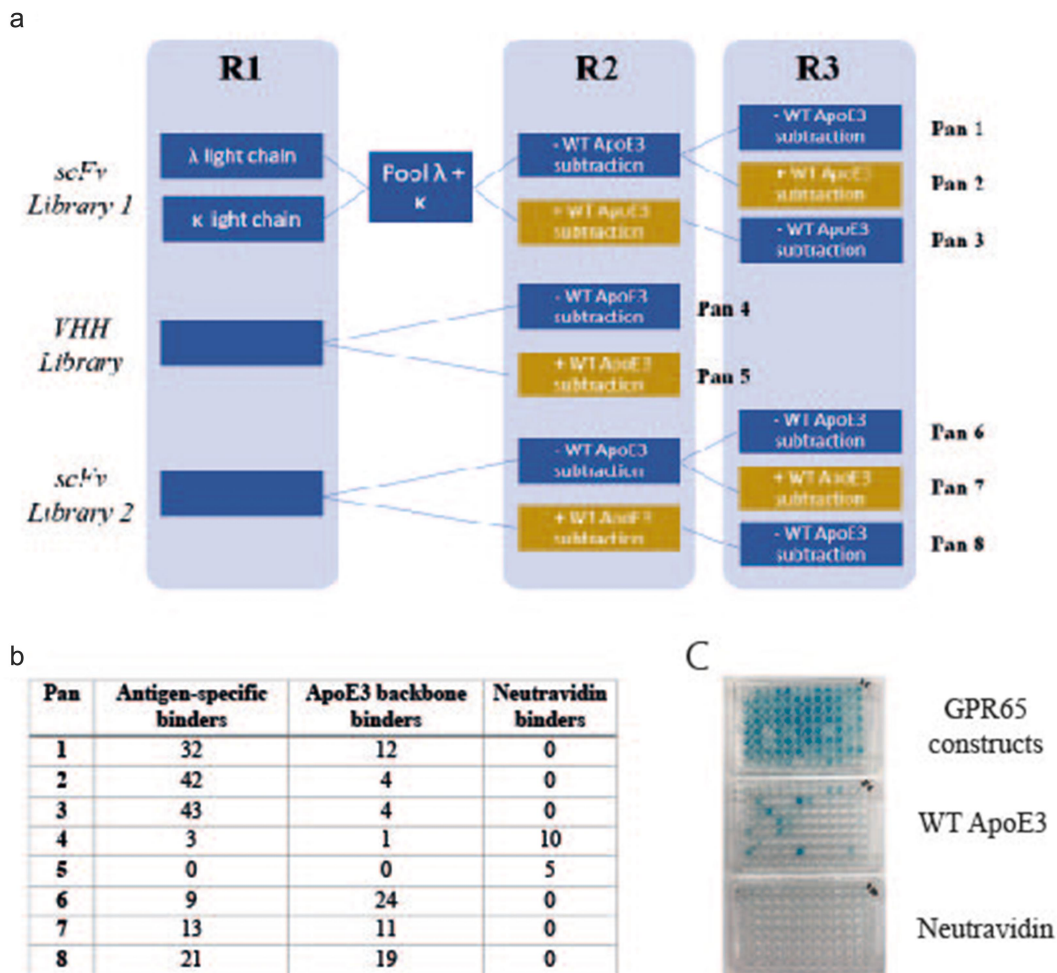


**Figure 2.** Generation of GPR65 antigen-specific monoclonal antibodies, using phage display. a) Schematic of phage display panning; three constructs representing each extracellular loop of GPR65 were pooled and acted as antigen throughout all stages of phage panning, for each of the three libraries screened (2 naïve scFv and naïve VHH). The antigen concentration remained the same throughout each round (1.5 $\mu$ M) and rounds 2 and 3 also included a subtraction step against WT ApoE3 (yellow boxes), to remove antibodies that bound the backbone. Eight pans were generated, each representing a different panning strategy. Phage antibody-containing supernatant was analyzed by ELISA against the pool of three chimeric constructs, WT ApoE3 and neutravidin. Those positive only on the construct plate were selected as antigen-specific hits, whilst those which also bound ApoE3 were deemed backbone binders. b) Binding results from each of the different panning conditions. c) Representative ELISA plates for pans 1 and 3 (half a plate each; pan 1 on the left-hand side, pan 3 on the right-hand side).

Upon phagemid DNA amplification by PCR, sequencing analysis identified 28 unique antibodies, 26 derived from the scFv libraries, and 2 from the VHH phage library. To screen for antibody activity, extracted VHH and scFv products were subjected to seamless cloning and reformatted into scFv-rabbit Fc or VHH-rabbit Fc formats; 20 phage antibodies were successfully cloned.

The antibodies were transiently expressed, and binding specificity verified by ELISA. Of the 17 antibodies successfully expressed, loop-specific antibodies were confirmed to have been generated, with 7 recognizing the ECL1 construct, whilst 10 bound the ECL2 construct

(Figure 3). Though expecting to see binding to ECL2 as the largest of the three loops, it was encouraging to also see binding to one of the smaller loops, ECL1.

A successful phage campaign delivered chimeric construct-specific antibodies, but it was important to understand whether these could recognize receptor expressed on a cell surface. Expression of both upstream FLAG and downstream GFP (Figure 4a, b) were used to imply surface expression of wild-type GPR65 upon being transiently transfected into HEK cells. In a primary binding screen on these cells, concentration-dependent binding to the receptor was observed for 3 of the phage-derived antibody-

	1	2	3	4	5	6	7	8	9	10	11	12
A	0.065	0.036	0.132	0.173	0.039	0.039	0.061	0.036	0.041	0.118	0.054	0.100
B	0.515	0.077	0.187	0.072	1.231	0.042	0.055	0.067	0.043	0.543	1.394	0.115
C	0.562	0.045	0.038	0.048	0.270	0.473	0.045	0.040	0.055	0.548	0.191	0.330
D	0.037	0.436	0.041	0.163	0.036	0.457	0.040	0.036	0.055	0.090	0.538	0.398
E	0.044	0.048	0.044	0.052	0.782	0.041	0.047	0.045	0.043	0.062	0.762	0.042
F	0.040	0.569	0.035	0.677	0.035	0.033	0.041	0.033	0.035	0.637	0.663	0.033
G	0.041	0.467	0.038	0.678	0.033	0.046	0.043	0.047	0.032	0.480	0.626	0.038
H	0.039	0.046	0.035	0.037	0.255	0.034	0.035	0.047	0.036	0.044	0.935	0.051
	ECL1			ECL2			ECL3			All		

**Figure 3.** Phage derived antibodies specifically bound ECL1 and ECL2 GPR65 chimeric constructs. 20 cloned antibodies were expressed, and antibody-containing supernatant binding was tested by ELISA against plate-bound individual chimeric constructs or as a pool, to determine their specificity (numbers provided are optical density values). Layouts of antibodies tested were repeated across the plate, per each binding profile (ECL1, ECL2, ECL3 and a pool of all three in 'All'). Binding is highlighted in green. The purple wells represent values from the secondary antibody control, the blue wells are blank controls, and the red values from mock transfected HEK cell supernatant, as an additional control.

containing supernatants, compared to background (Figure 4c, d). The three binders specifically recognized ECL2 and represented the two distinct libraries panned; Ab1.1 coming from the VHH library (pan 4, without WT ApoE3 subtraction), and antibodies Ab5.2 and Ab5.3 derived from scFv library 1. Indeed, Ab5.2 and Ab5.3 came from the same campaign (pan 1, without WT ApoE3 subtraction) but being discovered independently increases confidence in the validity of the sequence. The consistent performance of these two clones throughout screening, further confirms the binding profile of this antibody and supported selection for further interrogation.

To remove any unwanted signals from artifacts that may have been in the supernatant, the three GPR65-specific antibodies were purified by Protein A tips (Phynexus) and were confirmed to maintain binding to GPR65 expressed on HEK cells. Binding of these antibodies was then assessed against primary immune cell subsets, to verify binding to native receptor *ex-vivo*. At this stage, only Ab1.1 presented population right shifts of binding, which appeared to titrate out, on CD16<sup>+</sup> NK cells, B cells and monocytes, suggesting recognition of the receptor expressed on the surface of these cells; whilst not binding to T cells (Figure 5).

## Discussion

Here, chimeric antigens have been shown to be a viable approach to the discovery of antibodies to difficult membrane protein targets, through the display of GPR65 extracellular loops on a soluble scaffold.

Antibodies being used as tool reagents is not a new concept, with many specifically developed to understand target biology and function, or to aid with structural studies. There is currently no gold standard for antibody generation to any given target, with a broad variety of strategies used in campaigns, to leverage upon each of their advantages and disadvantages. Antibodies derived from antigen-specific B cells upon immunization of a host have already undergone affinity maturation, have a high specificity and provide low immunogenicity. Whilst display technologies offer the screening of large libraries covering millions of V(D)J combinations, compared to the circulating average  $10^7$  in humans, ultimately improving the chance of identifying rare antibodies [16,17].

Due to known difficulties of immunizing hosts with small epitope, membrane expressed proteins, identifying a GPR65 antibody through phage display was favored. For optimal success, the antigen being presented needs to be as similar to its native conformation as possible. Without reliable recombinant protein, screening against whole cells expressing the target is an alternative solution, particularly for GPCRs as native conformation is presented. However, this approach also has its own limitations. Low abundance of membrane protein expressed on cells, coupled with a high background of other proteins displayed on the surface of a cell do not create the best environment for identifying target-specific binders, particularly here where small extracellular domains were the site of interest. Moreover, phage particles are notoriously sticky and have been known to be

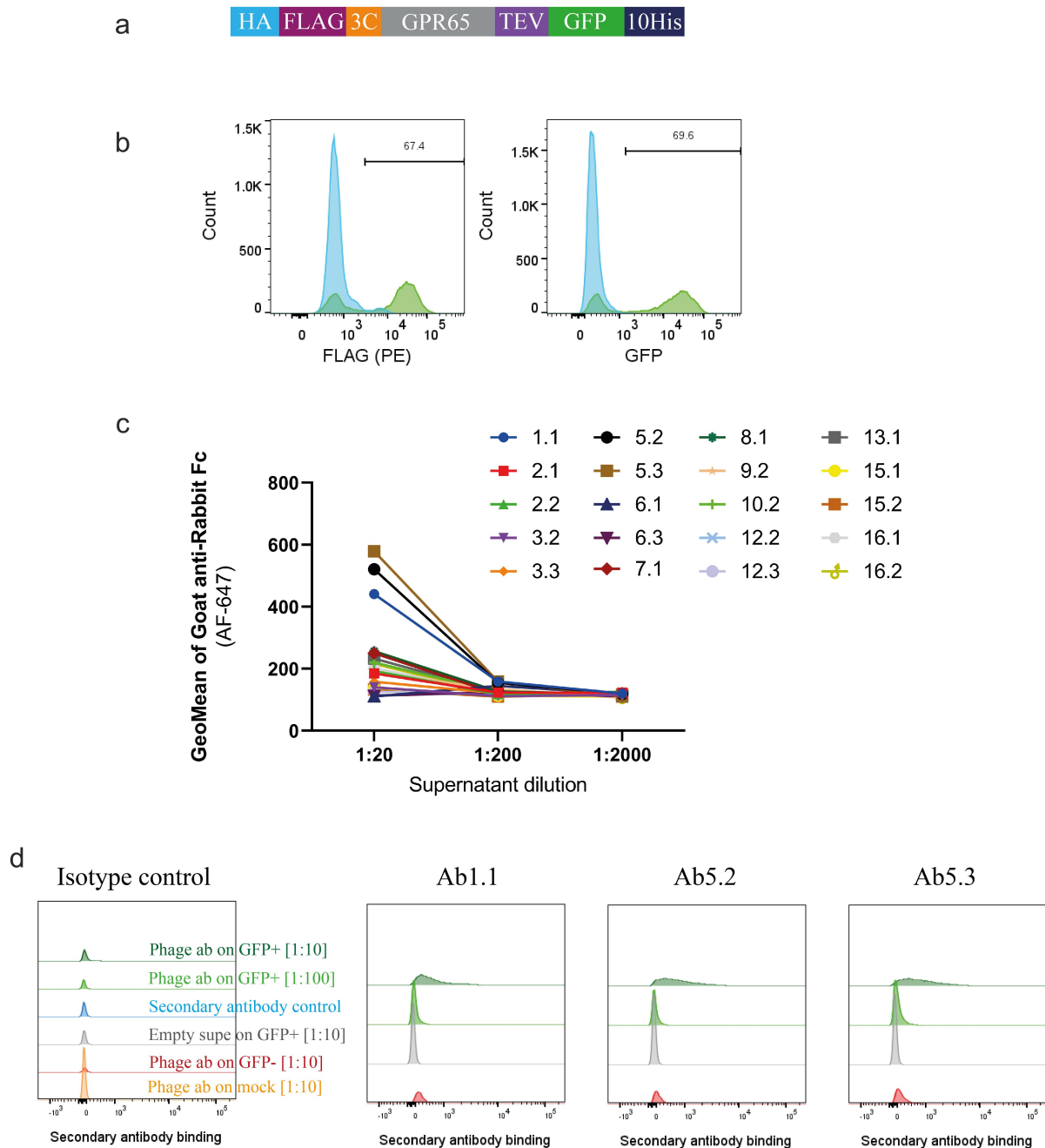


**Figure 4.** Phage-derived antibodies raised against chimeric constructs were able to recognise GPR65 expressed on HEK cells. a) GPR65 construct containing hemagglutinin (HA) signal sequence to encourage trafficking to the cell surface, FLAG tag to confirm surface expression, 3C and TEV protease sites to cleave off tags, His tag to aid with purification and GFP to aid with detection of gene expression. b) The construct was transiently transfected into HEK cells and incubated for 24 h. Binding was analyzed by flow cytometry, after initially gating on forward and side scatter, by FLAG expression, through a PE-conjugated anti-FLAG antibody, and detection of GFP. Wild type HEK cells are depicted in blue, whilst HEK cells transfected with human GPR65 are depicted in green. Percentage of GPR65 positive cells (green) is stated within the plots. Diluted phage-derived antibody-containing supernatant was incubated with HEK cells  $\pm$ GPR65, and binding was detected using an anti-rabbit Fc. c) Initial HEK cell screen of all phage-derived antibodies, highlighting 3 titrating GPR65-specific binders. d) Flow cytometry plots of the three GPR65-specific binders where GFP<sup>+</sup> cells represent GPR65 expressing cells (green), whilst GFP<sup>-</sup> cells (reg and grey) represent the internal negative control of cells not successfully transfected with GPR65 DNA, while mock cells (orange) reflect WT HEK cells having undergone the transfection protocol, without the addition of any DNA.

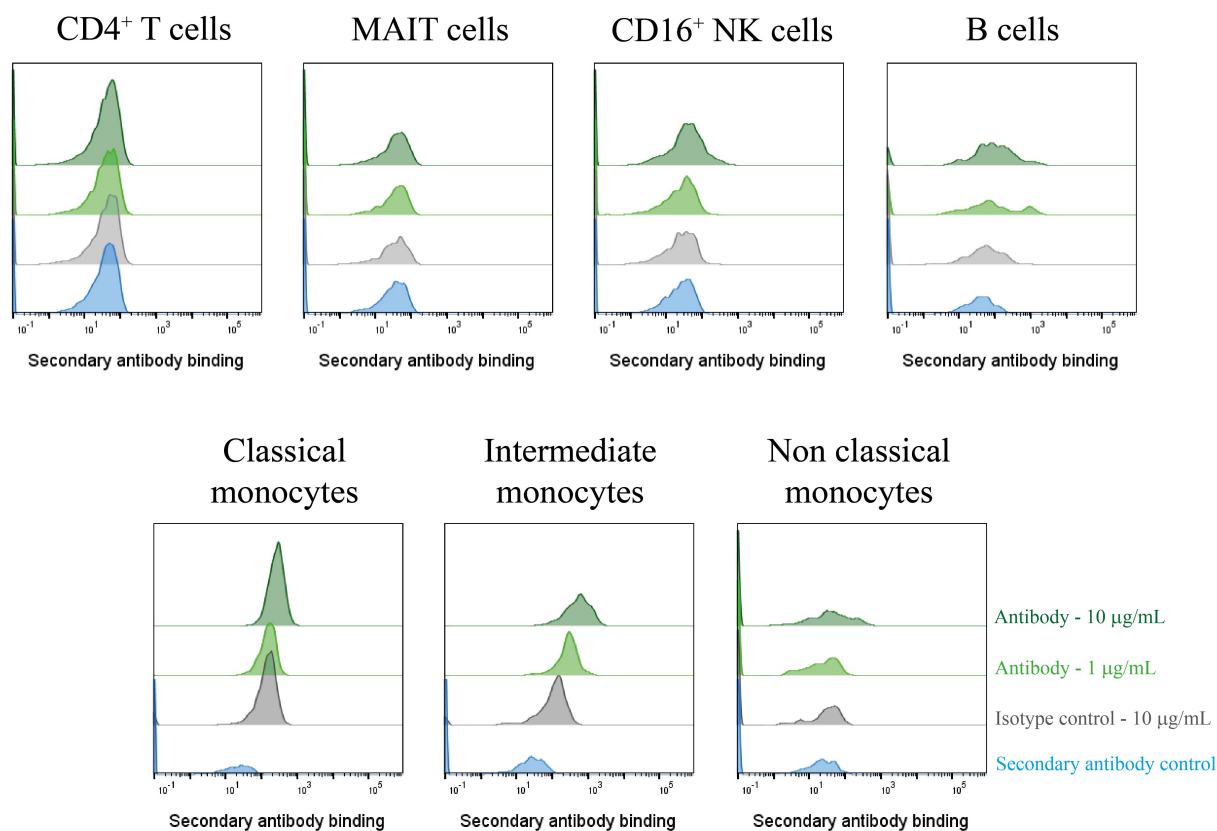


**Figure 5.** A GPR65-specific monoclonal antibody was successfully derived from phage display of a chimeric protein. PBMCs were isolated from a healthy control ( $n = 1$ ), treated with Fc block for 10 min, then phage-derived antibody incubated with the cells for 1 h. DAPI-negative live cell subsets were identified according to their phenotype<sup>1</sup> before secondary antibody (anti-rabbit IgG AF647) binding was assessed by flow cytometry. Phage-derived antibody binding is depicted in light or dark green, at 1  $\mu\text{g}/\text{mL}$  or 10  $\mu\text{g}/\text{mL}$  respectively, with the secondary antibody control depicted in blue, and the isotype control reflected in grey. Ab1.1 is the example shown.

internalized by cell membrane receptors [16], shrinking the library being screened. Thus, a novel strategy for antigen presentation is desired.

Mindful of the approach of Correia and colleagues [15], chimeric constructs were designed and wild type GPR65 extracellular loops were successfully displayed on the alpha-helix of soluble ApoE3, when substituted at the specific joining site between the loop and alpha-helix. The lack of solubility of those constructs where amino acids of the backbones were replaced with GPR65 residues, suggested an alteration to the structure of the scaffold. While it is possible that the additional residues could contribute directly to the insolubility (e.g., FNAVML and INLNLF, represented the longest addition of amino acids at both the ends of the loop substitution), it seems more likely that structural integrity of the chimeras was compromised, possibly causing the proteins to misfold and aggregate into inclusion bodies and

highlighting the importance of maintaining the integrity of the alpha helices.

We note that Koksall *et al.*, report an antibody scaffold mimetic (ASM) in which the N terminus and all three extracellular loops of CXCR4 were presented in the complementarity-determining region of an antibody [18]. It is perhaps somewhat fortuitous that the juxtaposition of the loops was sufficiently similar in the ASM for useful antibodies to be obtained. The method we describe here enables antibodies to individual loops to be obtained, and of course these individual loops can be presented in separate constructs and used for immunizations and panning in parallel. We also believe that splicing onto alpha helical scaffolds in ApoE3 is more relevant and structurally representative for GPCR antigens than being supported on the beta sheet of an antibody scaffold. Although we have no experience of double substitution into adjacent loops in ApoE3, we would

not necessarily advise following such an approach when using broadly for alternative GPCRs. Instead, one would recommend grafting each loop individually into separate ApoE3 frameworks, and possibly mixing as immunogens.

Within the human libraries screened, the multiple rounds of panning allowed for subtraction through enrichment, minimizing attrition at later stages. Overall, the phage display campaign was a success, with 17 antibodies discovered which bound the chimeric antigens, possessing specificity for the GPR65 substituted loops. It is of note, that pooling of antigens did not appear to bias antibodies dominant for one construct. Monoclonal antibodies recognizing both ECL1 and ECL2 were identified, whilst no antibodies were recovered for ECL3.

Without the ability to screen for binding to GPR65 recombinant protein, three phage-derived antibodies were shown to specifically recognize GPR65 expressed on HEK cells, with binding comparisons between the WT GPR65 receptor, alternative membrane proteins and mock-transfected cell lines; thus, validating the technique for using scaffold proteins to display antigen and elicit a response to facilitate the identification of native antigen-specific binders. However, for these antibodies to be useful for interrogating GPR65 biology, it was important they were able to bind endogenous receptor expressed on primary human cells.

We saw convincing binding of the VHH Ab1.1 to B cells, monocytes and NK cells, but not to CD4<sup>+</sup> T cells or mucosal-associated invariant T (MAIT) cells. To date, published data reporting GPR65 expression has been obtained through mRNA analysis, with MAIT cells, CD16<sup>+</sup> NK cells and non-classical monocytes as the highest expressors [19]. Through the inclusion of an Fc block step, the Fc portion of an antibody should have been prevented from interacting with FcγRIII (CD16) expressed on NK cells and non-classical monocytes.

The lack of binding at either concentration to MAIT cells was unexpected, although it is not unusual to observe discrepancies between mRNA and protein expression of a given target due to posttranscriptional processing and regulation [20]; therefore, transcripts are not sufficient to

predict protein levels [21]. However, if mRNA expression is high, there is a correlation for protein to be produced, even if not to the same high level. At the time of writing, there are no reports of GPR65 protein being expressed on MAIT cells. It is possible that the presentation and conformation of ECL2 in MAIT cells differs from other cell types, with potential occlusion of the loop from close binding of unreported proteins in a complex or differential glycosylation. In this context, it is of interest that Ab1.1 the VHH with the smallest footprint, showed binding to GPR65 on primary cells, while the scFv antibodies featuring larger paratopes were unable to bind. Further work is required to improve the antibody properties of Ab1.1, to be able to confidently use it as a tool reagent for probing GPR65 biology, in health and disease.

In addition, it is important to note that there is a potential N-linked site (NWT) in substituted ECL1 and another (NFT) in substituted ECL2 of the chimeric constructs, but it is not clear if these are used. Mammalian expression could readily be used for the expression of the chimeras, but variable and unrepresentative glycosylation could lead to antibodies with less than universal application in studies of native GPR65. Glycosylation can lead to occlusion of antibody-binding sites, but in this case antibodies, which bound to HEK expressed and primary cell GPR65 were discovered from panning against *E.coli*-produced constructs.

In summary, although applied so far to GPR65, the work presented here provides evidence to support a scaffold-based approach for displaying looped epitopes, resulting in the identification of native protein loop-specific antibodies. We see no reason why the method cannot be of general applicability with accurate, structurally enabled chimeras able to be readily constructed using the acceptor framework presented here. Not only does this technique provide promise for future display technology campaigns, but also within immunization strategies; using host species scaffolds to present targets with traditionally unstable structures to elicit a targeted immune response. With enhancements of research on basic structure, as well as developments of novel approaches for antibody discovery against difficult structures, the



generation of functional antibodies against difficult to target GPCRs is closer than ever before.

## Methods

### Chimeric protein expression and purification

Genes encoding ApoE3 chimeric constructs were synthesized by ATUM, and cloned into BamHI and NcoI restriction sites of a pET14b vector. These constructs were co-transformed with a pRSFDuet-1 vector encoding Biotin ligase BirA, into NiCo21(DE3) *E. coli* cells (New England Biolabs). Expression and purification of the constructs were performed, as described by the Swanstrom lab [22], with addition of 100  $\mu$ M biotin to the growth medium at the time of induction with IPTG. Protein concentration was determined on a Nanodrop spectrophotometer, using absorption at 280 nm (Thermo Scientific). To determine the solubility of each protein upon expression in *E. coli*, SDS-PAGE was performed. Briefly, samples taken from the cultures, before and after induction, were lysed using BugBuster MasterMix. After taking a sample from the lysate of the induced culture sample, it was further separated in a soluble and insoluble fraction by centrifugation. NuPAGE™ LDS Sample Buffer 4 $\times$  (Invitrogen) containing dithiothreitol (Invitrogen), was added to cell lysates, soluble protein fraction and insoluble protein pellets to a final 1X concentration, before being run along a NuPAGE™ 4–12% Bis-Tris Protein Gel (Invitrogen). Instant blue™ (Expedeon) was used to reveal protein bands.

### Phage panning in solution

Three UCB established phage libraries were used; two naïve human scFv phage libraries and a naïve VHH phage library.

In the first round of panning, ApoE3 GPR65 loop constructs (1.5  $\mu$ M) were pooled and incubated with each library, previously blocked in PBS containing 3% milk. Constructs and associated phage were captured from solution using Sera-Mag™ SpeedBeads Neutravidin-coated (GE Life Sciences). Beads were washed by magnetic capture 5 times with PBS + 0.1% TWEEN

(VWR), and bound phage were eluted by 100  $\mu$ g/mL trypsin (Sigma) in Tris-buffered saline buffer. Mid-log growing TG1 cells were infected with these phage particles and used for output titrations and overnight amplification. Rescued phage from round one was split in two and incubated directly with either the same pool of antigen, or 1.5  $\mu$ M WT ApoE3 construct, to remove binders to the ApoE3 scaffold. Complexes were captured using Dynabeads™ M-280 Streptavidin (Invitrogen), to remove neutravidin binders, followed by selection on chimeric ApoE3 GPR65 proteins. Enriched phage from round two of both human libraries were subject to a final round, and complexes were captured with neutravidin beads. As the VHH library was smaller than the human libraries, only two rounds of panning were carried out. Phage rescue was performed from polyclonal *E. coli* populations between rounds or from individual *E. coli* colonies after the final round.

### Phage rescue

Phage rescue was performed using a modification of the standard protocol [23]. Cultures were seeded at a starting density of 0.1 OD<sub>600</sub> in 2 $\times$ YT medium with 2% glucose and 100  $\mu$ g/mL carbenicillin and grown at 37°C with shaking at 220 rpm until the OD<sub>600</sub> reached between 0.4 and 0.8. The culture was then infected with M13KO7 at a multiplicity of infection of 10 and incubated at 37°C for 1 h, without shaking. The culture was then centrifuged at 4000 rpm for 10 min. The pellets were resuspended in 100 mL 2 $\times$ YT containing 100  $\mu$ g/mL carbenicillin and 50  $\mu$ g/mL kanamycin. These cultures were grown for 18 h at 30°C, shaking at 240 rpm. Next, the cultures were centrifuged at 8000 rpm for 15 min and phage-containing supernatants were used for ELISA screening or precipitated for further selection rounds through incubation with 7 mL PEG sodium chloride for 1 h, on ice.

### Phage antibody characterisation and optimisation

Monoclonal phage antibodies were screened for binding to the antigen they were raised against, WT ApoE3 and neutravidin, by ELISA. Briefly, biotinylated antigen (chimeric constructs and WT ApoE3) or

neutravidin was coated onto ELISA plates at 1 µg/mL. Plates were blocked with PBS with 3% milk (Sigma), before 100 µL of pre-blocked phage supernatant was applied to the plate. Following a wash step (composition of ELISA wash is detailed in Supplementary Table S1), anti-M13 HRP (Sino Biological) was added at 1:15000 dilution. Plates were developed with TMB, before being read at 630 nm, on Synergy 2 (BioTek).

Phagemid DNA was sequenced (Macrogen), before unique scFv/VHH regions were extracted, amplified, and reformatted into a rabbit Fc fusion vector, by seamless cloning (GeneArt™ Seamless Cloning and Assembly Enzyme Mix).

The unique antibodies were synthesized and cloned into custom vectors by TWIST Bioscience.

### **DNA constructs and preparations**

A human GPR65 DNA construct was designed (Uniprot entry Q8IYL9) along with a N-terminal FLAG tag, a C-terminal 10-histidine tag and labeled with GFP. Custom synthesis and cloning into a mammalian expression vector were performed by ATUM (California, USA). Plasmid DNA was amplified through Qiagen Plasmid Plus Giga kits and quantified.

### **Antibody and target transient expression**

HEK293 cells were cultured in EXPI293 expression media (Life Technologies), and cell concentration and viability were determined using trypan blue (Gibco, Life Technologies). Cells were routinely cultured at 37°C, in 8% CO<sub>2</sub>, in vented Erlenmeyer flasks (Corning, Surrey, UK), shaking at 180 rpm and sub-cultured every 3–4 days, at a seeding density of  $0.5 \times 10^6$  cells/mL.

Cells were transfected with DNA-lipid complexes comprising DNA and Expifectamine293 (Life Technologies) at a 1 µg DNA:1 or  $3 \times 10^6$ /mL cell ratio for target and antibodies, respectively, and prepared according to manufacturer's protocol. Transfected cells were incubated for 24 h, or up to 7 days, respectively, prior to use.

### **Isolation of peripheral blood mononuclear cells (PBMCs)**

Venous blood samples from anonymous healthy donors based at UCB Celltech, Slough, UK were taken directly into heparin-containing tubes. Blood samples were taken with informed consent under UCB Celltech HTA License number 12,504, as approved by the Human Tissue Authority. All donors gave written informed consent in accordance with the Declaration of Helsinki.

Sample was diluted 1:1 with PBS and mononuclear cells were separated from whole blood using Leucosep™ tubes. These were centrifuged at 800×g for 15 min with no brake, and the PBMC-containing interface was collected using a Pasteur pipette. Cells were washed twice in PBS containing 1 mM EDTA (here on in referred to as PBS +EDTA) for 10 min at 200×g, then resuspended in R10. Cells were counted after staining with trypan blue using a hemocytometer under a light microscope.

### **Flow cytometry**

Monoclonal antibodies used here are listed in Supplementary Table S2. Data acquisition was obtained using a BD Bioscience Canto II. Fluorescence was compensated using single color compensations Ultracomp beads (eBioscience) and data were analyzed using FlowJo v9 or newer (BD Life Sciences).

### **Surface staining**

Up to  $2 \times 10^5$  cells/well were stained in FACS buffer (composition of buffer is detailed in Supplementary Table S1), in a total volume of 50 µL per well. Cells were incubated for up to 1 hour at 4°C in the dark with a panel of fluorochrome conjugated antibodies. Samples were then washed twice in FACS buffer and resuspended in up to 200 µL for acquisition (with DAPI (Biolegend)).

Where primary and secondary antibodies were used, cells were first stained with the primary antibody as described above, washed twice in FACS buffer, and

stained with secondary antibody for a further 30 min. Instances where Fc block (BD Biosciences) was used,  $2.5 \mu\text{g}/1 \times 10^6$  cells was added for 10 min prior to surface antibody incubation.

## Abbreviations

ApoE3	Apolipoprotein E 3
AS	Ankylosing spondylitis
CCR4	C-C chemokine receptor 4
DNA	Deoxyribonucleic acid
ECL	Extracellular loop
ELISA	Enzyme-linked immunosorbent assay
FDA	Food and Drug Administration
GFP	Green fluorescence protein
GPCR	G-protein coupled receptor
HEK	Human embryonic kidney 293 cells
ICL	Intracellular loop
MAIT	Mucosal-associated invariant T cell
mRNA	Messenger ribonucleic acid
NK cell	Natural killer cell
PBMC	Peripheral blood mononuclear cells
PCR	Polymerase chain reaction
scFv	Single chain variable fragment
VHH	Single variable domain on a heavy chain
WT	Wild type

## Note

1. CD4<sup>+</sup> T cells = CD3<sup>+</sup>, CD4<sup>+</sup>  
MAIT cells = CD3<sup>+</sup>, CD8<sup>+</sup>, CD161<sup>+</sup>, V $\alpha$ 7.2<sup>+</sup>  
CD16<sup>+</sup> NK cells = CD3<sup>-</sup>, CD56<sup>+</sup>, CD16<sup>+</sup>  
B cells = CD3<sup>-</sup>, CD19<sup>+</sup>  
Classical monocytes = CD3<sup>-</sup>, CD14<sup>+</sup>, CD16<sup>-</sup>  
Intermediate monocytes = CD3<sup>-</sup>, CD14<sup>+</sup>, CD16<sup>+</sup>  
Non-classical monocytes = CD3<sup>-</sup>, CD14<sup>-</sup>, CD16<sup>+</sup>

## Acknowledgments

We thank Anthony Scott-Tucker for helpful advice surrounding phage display strategy.

## Disclosure statement

No potential conflict of interest was reported by the author(s).

## Funding

The work described here was funded by UCB Pharma, with the following authors current employees Janine Barrett, Seppe Leysen, Cécile Galmiche, Thomas E. Edwards, Alastair D.G. Lawson, and Hussein Al-Mossawi a previous employee.

ADGL and TEE hold shares and/or share options in UCB Pharma.

PB received support from the NIHR Oxford Biomedical Research Centre (BRC). The views expressed are those of the author(s) and not necessarily those of the NHS, the NIHR or the Department of Health.

## Data availability statement

The data that support this study are available from the corresponding author, JB, upon reasonable request.

## Additional Information

This work was supported by UCB Pharma; no further funding was received.

## Author contributions

JB designed and carried out experiments, analyzed and interpreted data, and wrote the manuscript. SL, CG and ADGL contributed to the concept of the work, designed experiments, interpreted data and contributed to writing the manuscript. TEE, HA-M and PB contributed to the concept of the work and contributed to writing the manuscript.

## ORCID

Janine Barrett  <http://orcid.org/0009-0009-5984-4690>

## References

- [1] Dougados M, Baeten D. Spondyloarthritis. *Lancet*. 2011;377(9783):2127–2137. doi: 10.1016/S0140-6736(11)60071-8
- [2] Navarro-Compán V, Sepriano A, El-Zorkany B, et al. *Axial spondyloarthritis*. *Ann Rheum Dis*. 2021;80(12):1511–1521. doi: 10.1136/annrheumdis-2021-221035
- [3] Lambert RG, Salonen D, Rahman P, et al. Adalimumab significantly reduces both spinal and sacroiliac joint inflammation in patients with ankylosing spondylitis: a multicenter, randomized, double-blind, placebo-controlled study. *Arthritis Rheum*. 2007;56(12):4005–4014. doi: 10.1002/art.23044
- [4] van der Heijde D, Gensler LS, Deodhar A, et al. Dual neutralisation of interleukin-17A and interleukin-17F with bimekizumab in patients with active ankylosing spondylitis: results from a 48-week phase IIb, randomised, double-blind, placebo-controlled, dose-ranging study. *Ann Rheum Dis*. 2020;79(5):595–604. doi: 10.1136/annrheumdis-2020-216980
- [5] Cortes A, et al. Identification of multiple risk variants for ankylosing spondylitis through high-density genotyping of immune-related loci. *Nat Genet*. 2013;45(7):730–738. doi:10.1038/ng.2667

- [6] Ellinghaus D, Baurecht H, Esparza-Gordillo J, et al. High-density genotyping study identifies four new susceptibility loci for atopic dermatitis. *Nat Genet.* 2013;45(7):808–12. doi: [10.1038/ng.2642](https://doi.org/10.1038/ng.2642)
- [7] Choi JW, Lee SY, Choi Y. Identification of a putative G protein-coupled receptor induced during activation-induced apoptosis of T cells. *Cell Immunol.* 1996;168(1):78–84. doi: [10.1006/cimm.1996.0051](https://doi.org/10.1006/cimm.1996.0051)
- [8] Wang JQ, Kon J, Mogi C, et al. TDAG8 is a proton-sensing and psychosine-sensitive G-protein-coupled receptor. *J Biol Chem.* 2004;279(44):45626–33. doi: [10.1074/jbc.M406966200](https://doi.org/10.1074/jbc.M406966200)
- [9] Kyaw H, ZENG Z, SU K, et al. Cloning, characterization, and mapping of human homolog of mouse T-cell death-associated gene. *DNA Cell Biol.* 1998;17(6):493–500. doi: [10.1089/dna.1998.17.493](https://doi.org/10.1089/dna.1998.17.493)
- [10] Hauser AS, Attwood MM, Rask-Andersen M, et al. Trends in GPCR drug discovery: new agents, targets and indications. *Nat Rev Drug Discov.* 2017;16(12):829–842. doi: [10.1038/nrd.2017.178](https://doi.org/10.1038/nrd.2017.178)
- [11] Hutchings CJ. Mini-review: antibody therapeutics targeting G protein-coupled receptors and ion channels. *Antib Ther.* 2020;3(4):257–264. doi: [10.1093/abt/tbaa023](https://doi.org/10.1093/abt/tbaa023)
- [12] King CT, Gegg CV, Hu SN-Y, et al. Discovery of the migraine prevention therapeutic aimovig (erenumab), the first FDA-Approved antibody against a G-Protein-coupled receptor. *ACS Pharmacol Transl Sci.* 2019;2(6):485–490. doi: [10.1021/acsptsci.9b00061](https://doi.org/10.1021/acsptsci.9b00061)
- [13] Niwa R, Shoji-Hosaka E, Sakurada M, et al. Defucosylated chimeric anti-CC chemokine receptor 4 IgG1 with enhanced antibody-dependent cellular cytotoxicity shows potent therapeutic activity to T-cell leukemia and lymphoma. *Cancer Res.* 2004;64(6):2127–33. doi: [10.1158/0008-5472.CAN-03-2068](https://doi.org/10.1158/0008-5472.CAN-03-2068)
- [14] Ishida T, Iida S, Akatsuka Y, et al. The CC chemokine receptor 4 as a novel specific molecular target for immunotherapy in adult T-Cell leukemia/lymphoma. *Clin Cancer Res.* 2004;10(22):7529–39. doi: [10.1158/1078-0432.CCR-04-0983](https://doi.org/10.1158/1078-0432.CCR-04-0983)
- [15] Correia BE, Bates JT, Loomis RJ, et al. Proof of principle for epitope-focused vaccine design. *Nature.* 2014;507(7491):201–6. doi: [10.1038/nature12966](https://doi.org/10.1038/nature12966)
- [16] Chan CE, Lim APC, MacAry PA, et al. The role of phage display in therapeutic antibody discovery. *Int Immunol.* 2014;26(12):649–657. doi: [10.1093/intimm/dxu082](https://doi.org/10.1093/intimm/dxu082)
- [17] Kumar R, Parrray HA, Shrivastava T, et al. Phage display antibody libraries: a robust approach for generation of recombinant human monoclonal antibodies. *Int j biol macromol.* 2019;135:907–918. doi: [10.1016/j.ijbiomac.2019.06.006](https://doi.org/10.1016/j.ijbiomac.2019.06.006)
- [18] Koksai AC, et al. Functional mimetic of the G-protein coupled receptor CXCR4 on a soluble antibody scaffold. *Mabs.* 2019;11(4):725–734. doi: [10.1080/19420862.2019.1596703](https://doi.org/10.1080/19420862.2019.1596703)
- [19] Stephenson E, Reynolds G, Botting RA, et al. Single-cell multi-omics analysis of the immune response in COVID-19. *Nat Med.* 2021;27(5):904–916. doi: [10.1038/s41591-021-01329-2](https://doi.org/10.1038/s41591-021-01329-2)
- [20] Buccitelli C, Selbach M. mRnas, proteins and the emerging principles of gene expression control. *Nat Rev Genet.* 2020;21(10):630–644. doi: [10.1038/s41576-020-0258-4](https://doi.org/10.1038/s41576-020-0258-4)
- [21] Liu Y, Beyer A, Aebersold R. On the dependency of cellular protein levels on mRNA abundance. *Cell.* 2016;165(3):535–550. doi: [10.1016/j.cell.2016.03.014](https://doi.org/10.1016/j.cell.2016.03.014)
- [22] Zhu C, Dukhovlina E, Council O, et al. Rationally designed carbohydrate-occluded epitopes elicit HIV-1 Env-specific antibodies. *Nat Commun.* 2019;10(1):948. doi: [10.1038/s41467-019-08876-w](https://doi.org/10.1038/s41467-019-08876-w)
- [23] Marks JD, Hoogenboom HR, Bonnert TP, et al. Bypassing immunization. Human antibodies from V-gene libraries displayed on phage. *J Mol Biol.* 1991;222(3):581–97. doi: [10.1016/0022-2836\(91\)90498-U](https://doi.org/10.1016/0022-2836(91)90498-U)

# AbNano™ VHH Naïve Library

## Overview

AbNano™ VHH Naïve Library from Fortis Life Sciences® is a fully natural, single domain naïve library derived from camelid source material and the antibodies displayed on monovalent phage. It is intended for research purposes to aid in the discovery of antibodies intended for use as therapeutics, diagnostics, and research tools.


## Why select the AbNano™ VHH Naïve Library

- **Save 18 weeks** by starting with a prepared library that is ready to pan
- To **maximize diversity**, this library was constructed from 103 naïve animals: 77 llamas and 26 alpacas.  $1.51 \times 10^{10}$  PBMC cells were collected and used for library construction and the total number of transformants for the library was  $1.12 \times 10^{10}$  cfu.
- Naïve library can potentially **bind a high number of targets** compared to single-animal or single-target libraries
- This **fully natural library** has higher diversity in framework regions than synthetic libraries
- Lower affinity is ideal for the engineering of **multispecific antibodies or self-assembling therapeutics**
- **Data package included** to support utility in identifying binders for several popular targets

Learn more by visiting [fortislife.com/products/abnano-vhh-libraries](https://fortislife.com/products/abnano-vhh-libraries)



## Development and Utilization of VHH Antibodies Derived from *Camelus Dromedarius* Against Foot-and-Mouth Disease Virus

Lipsa Dash<sup>a</sup> , Saravanan Subramaniam<sup>a</sup>, Sagar A. Khulape<sup>a</sup>, Bikash Ranjan Prusty<sup>a</sup>, Kamal Pargai<sup>a</sup>, Shirish D. Narnaware<sup>b</sup>, Niteen V. Patil<sup>b</sup> and Bramhadev Pattnaik<sup>a</sup>

<sup>a</sup>ICAR-Directorate on Foot and Mouth Disease, Mukteswar, Nainital, Uttarakhand, India; <sup>b</sup>ICAR-National Research Center on Camel, Jorbeer, Bikaner, Rajasthan, India

### ABSTRACT

Foot-and-mouth disease (FMD) is an acute, highly contagious, and economically devastating viral disease of domestic and wildlife species. For effective implementation of FMD control program, there is an imperative need for developing a rapid, sensitive, and specific diagnostics which help in the identification of serotypes involved in the outbreaks. The humoral immune response of the Camelidae is unique since in these animals 75% of circulating antibodies are constituted by heavy-chain antibodies and 25% are conventional immunoglobulin with two identical heavy chains. In the present study, we developed and characterized FMD virus-specific single-domain heavy-chain antibodies (VHHs) against inactivated whole-virus antigens of FMDV serotypes O (INDR2/1975), A (IND40/2000), and Asia 1 (IND63/1972) vaccine strains. After six rounds of panning and enrichment, these VHHs were stably expressed in *Escherichia coli* cells. The VHHs directed against outer capsid proteins of FMD virus were successfully utilized as the capture antibody in liquid-phase blocking ELISA (LPBE) thus replacing rabbit coating antibodies. Our study demonstrated the utility of FMD virus-specific VHHs as potential candidates in FMD research and diagnostic application.

**Abbreviations:** 2XYT: Amp-Glu medium; CDR: complementary determining regions; DAS-ELISA: double-antibody sandwich ELISA; FR1: framework region 1; FR2: framework region 2; LB agar: Luria Bertani agar; OPD: Orthophenylene-diamine dihydrochloride; PBS: phosphate-buffered saline; PBST: phosphate-buffered saline with Tween20; SMP: skimmed milk powder; TRX: Thioredoxin tag

### KEYWORDS

ELISA; FMDV; heavy-chain antibodies; immune library

### Introduction

Foot-and-mouth disease (FMD) is a highly contagious and economically devastating viral disease of diverse artiodactyls species like cattle, buffaloes, pigs, sheep, goats, elephants, and more than 30 wild ungulates. It constitutes one of the main animal health concerns. Apart from direct losses, FMD indirectly hamper national and international trade and by decreasing the value of animal products. For effective implementation of FMD control program (FMD-CP), there is a requirement for prompt, sensitive, and specific laboratory diagnosis. The variable heavy-chain antibody fragments (VHHs) found only in camels, llamas, and shark (1) are being explored for diagnostic and therapeutic applications. The VHH consists of two heavy chains and devoid of light chains and CH1 domain found in conventional antibodies. The VHHs have distinct advantages over other recombinant fragments such as Fabs and scFvs, which include higher thermostability, solubility, and

smaller size required for effective cell penetration (2). The VHH can be produced through easy one-step cloning as a single polypeptide chain of size < 15 kDa.

The characteristic properties of VHHs can make the detection system based on them more specific and user-friendly pertaining to its stability, ease of production, and simplification of techniques for large-scale serosurveillance and seromonitoring toward FMDV control. The study was designed with the objective of development of VHHs specific to three FMD virus serotypes (O, A, and Asia1) endemic to India and exploiting them in ELISA-based diagnostic test to replace conventional rabbit serum as a coating antibody.

### Materials and methods

#### Blood collection and lymphocyte separation

Approximately 100 ml of blood samples was collected in heparinized vacutainer from three ~4-year-old female

camels (*Camelus dromedarius*) immunized with FMDV serotype O (INDR2/75), A (IND40/00), and Asia1 (IND63/72) whole-virus antigen. The animals maintained at an organized camel herd were tested to be negative for FMDV-nonstructural protein antibody (DIVA negative). The peripheral blood mononuclear cells (PBMCs) were separated from blood using Histopaque-1077 (Sigma-Aldrich, USA) centrifugation method as per the protocol (3).

### Amplification of VHH

Total RNA was extracted from the PBMCs using Trizol reagent (Sigma-Aldrich, USA) and mRNA was separated from the total RNA using Oligotex mRNA purification kit (Qiagen, Germany) as per the manufacturer's instructions. cDNA was synthesized from approximately 2 µg of mRNA from each camel in 25 µl reactions using Superscript II reverse transcriptase enzyme (Invitrogen, USA) and OligodT (12–18) primer. The VHH gene segment was amplified by Hi-Fi Platinum Taq (Invitrogen, USA) using nested PCR (Fig. 1) as a protocol detailed earlier (4).

### Cloning and library construction

The amplified product with inbuilt restriction site (*Pst*I and *Not*I, NEB Biosciences, USA) was cloned in phagemid expression vector pMECS (kindly gifted by Dr. Muyltermans). The ligated product was chemically transformed into the competent *Escherichia coli* TG1

cells (Stratagene) and positive colonies were selected by plating onto the LB agar plates containing ampicillin and glucose. The libraries of positive colonies were generated as per method described earlier (5).

### Selection of phage displayed VHH

Precipitated phage particles were titrated and subjected to panning against purified FMDV serotype O, A, and Asia1 vaccine strains. Antigens were coated overnight at 4°C in 96-well flat-bottomed immunoplates (NUNC-MaxiSorp, Denmark) at a concentration of 100 µg/ml using 50 mM sodium carbonate buffer, pH 9.6. The plates were blocked with 2% SMP in PBST at room temperature for 2 h washed thrice with PBS before the addition of  $3 \times 10^{12}$  phages for the first round of panning. After 90 min of incubation at room temperature, the wells were washed 10 times with PBS 0.05% Tween, bound phages were eluted with 0.1 M triethylamine (Sigma-Aldrich, USA), pH 11.0. Eluted phages were titrated, used to infect TG1 cells and plated on 2XYT ampicillin, glucose agar plates. The same complete procedure was repeated for four rounds of panning. In each round of panning, the enrichment of the phage sublibrary obtained was calculated as the ratio of output/input phages. The periplasmic extract of 96 single individual colonies of bacteria for each antigen, picked randomly were screened using periplasmic extract ELISA (PE-ELISA) for checking the reactivity. For this, FMDV serotypes O, A, and Asia1 of purified 146S particle were coated onto 96-well microtiter plates and were incubated overnight at 4°C. The plates were blocked with PBST buffer (5% skim milk, 10% *E. coli* lysate with 0.05% Tween 20) at room temperature for 1 h. The periplasmic extracts were then added to the plates and incubated for 1 h at room temperature. After this incubation period, mouse anti-His tag antibody (GE Healthcare, USA), at a dilution of 1:2000, was added, followed by antimouse horseradish peroxidase conjugate (Dako, Denmark). The reaction was developed with OPD and H<sub>2</sub>O<sub>2</sub> substrate and was stopped with 2.0 M sulfuric acid. The optical absorbance was measured at 492 nm.

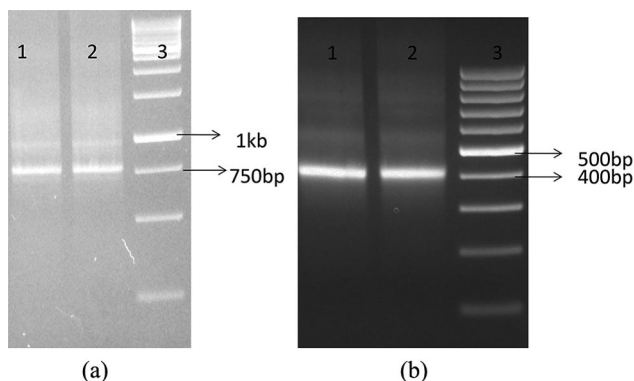


**Figure 1.** Nested PCR strategy for amplification of VHH segment. (a) This figure represents the amplification products of the 1st strand cDNA PCR containing fragments with two different sizes. Lanes 1 and 2: Outer PCR amplification of 900 bp region of VH-CH1-Hinge-CH2; 750 bp region of VHH-short Hinge of IgG2-CH2 and complete VHH segment with long hinge of IgG3 and part of CH2. Lane 3: 1 kb molecular marker (Thermo scientific U.S.A), and (b) Lanes 1 and 2: Inner PCR amplification of 400 bp VHH only. Lane 3: 100 bp molecular marker (Thermoscientific, USA).

### Sequencing of VHH library

The nucleotide sequencing was performed using VHH-specific forward and reverse primer in AB13130 capillary sequencer (Applied Biosystems) for the selected clones. The deduced amino acid sequences were aligned using Clustal W to detect variations within the CDR regions of the VHH.

### Optimization of expression of VHH in prokaryotic system

For expression of VHHs, one clone each of serotypes O, A, and Asia1 which showed strong reactivity in PE-ELISA were chosen and cloned into pET32 expression vector and into RosettaGami(DE3) pLacI *E. coli* cells (Novagen). Trx-His-tagged VHHs were expressed by induction with 1 mM IPTG at 28°C for 6 h. His-tagged VHH was expressed by the addition of 1 mM IPTG at 28°C for 6 h. Expressed fused VHH was purified on NiNTA column (Qiagen, Germany) and was analyzed on 15% SDS-PAGE.

### Utilization of VHHs as coating antibody

The expressed VHHs were tested in DAS-ELISA to check the level of cross-reactivity as well as to finalize the optimum concentration to be used as coating antibodies by checkerboard titration against respective antigen. For this, 96-well microtiter plates were coated with different concentrations of recombinant anti-146S type-specific VHHs against FMDV O, A, and Asia 1 in coating buffer (carbonate/bicarbonate, pH 9.6) in 50 µl volumes. Coated plates were then kept at 4°C overnight. Inactivated FMDV serotypes O, A, and Asia1 viral antigens at a fixed concentration were added into the wells. For tracing the bound antigen, three FMDV serotype-specific guinea pig antisera were added to the corresponding wells including positive controls. The HRP-conjugated rabbit anti-guinea pig HRP IgG (Dako, Denmark) was added to all wells. After colorimetric reaction with OPD as a substrate, the reaction was stopped with 2.0 M sulfuric acid, and the absorbance was measured at 492 nm. After initial standardization, the recombinant VHHs were used as the capture antibody in liquid-phase blocking ELISA (LPB-ELISA) user for seromonitoring and serosurveillance of FMD in India (6). The aim was to replace the type-specific rabbit antibodies used in LPB-ELISA for capturing FMDV antigen with the recombinant VHHs. The assay was validated by screening bovine serum samples ( $n = 1023$ ) simultaneously in the modified and standard LPB-ELISA. The samples were taken from National FMD Virus Repository. The samples consisted of bovine samples of NDRI, Karnal where the cattle herd which was well maintained and vaccinated had an outbreak in 2012, serum samples were collected within 7 days of outbreak. Random bovine serum samples ( $n = 1023$ ) of age 2 years and above which were earlier tested by in-house LPB ELISA protocols of known status were subjected for DAS ELISA for validation of the test.

## Results and discussion

The aim of this current study was to isolate higher affinity VHHs to FMDV serotypes O, A, and Asia1 structural proteins (146S particles) by constructing an immune phage-displayed VHH library. Thus, these recombinant VHHs can replace the conventional rabbit serum as the capture antibody in ELISA-based diagnostic assays.

### Immunization of camels

The immunized camels generated polyclonal response against BEI-inactivated FMDV 146S particles. After third booster on 49th day, the serum titers were >1:2048, >1:1024, >1:4096, respectively, for FMD virus serotypes O, A, and Asia1.

### Generation of library

The mRNA extracted from PBMC was subjected to nested PCR amplification to obtain VHH segment (Fig. 1). The 400 bp amplified products were cloned in pMECS phagemid vector to develop VHH library. Following amplification and cloning of the VHH gene repertoire into the pMECS phagemid vector, the ligated product was transformed into the freshly prepared electrocompetent cells of *E. coli* TG1 strain by electroporation to maintain and propagate the library.

### Phage selection by panning

Screening of phage display libraries is usually done by an affinity selection (or biopanning) during which phage populations are exposed to targets to selectively capture binding phage. There was enrichment of antigen-specific phage antibodies directed against FMDV after only two rounds of panning while the majority of enrichments occurred during the third and fourth rounds of panning. Variable levels of enrichment were noted during sequential rounds of biopanning. More the rounds of panning, diversity decreases, but specific VHH population increases, thus six rounds of panning were performed to select VHHs with higher affinity or to bias the selection to a specific epitope of interest for all three proteins (5).

### Screening of antigen binders

In PE-ELISA, the colony was considered positive only if the absorbance in the antigen-coated well was at least twofold that of the noncoated negative control well. After three rounds of panning, the PE-ELISA showed



good binding signal and about 60–70% of individual phage clones showed specific binding to serotypes O, A, and Asia1 antigen thus indicating enrichment for various FMDV binders. Overall, 17 colonies corresponding to serotype O, 26 for serotype Asia 1, and 27 for serotype A showed reactivity in PE-ELISA, divided into groups as strong, medium, and weak positives with respect to their absorbance intensities.

### Sequence diversity

The nucleotide sequences of VHH were determined from 52 clones which were PE-ELISA positive to determine the quality and heterogeneity of the library. The nucleotide blast analysis using the blast tool of NCBI showed several sequence hit with available VHH sequences mostly in the FR region. At the end of the third round of panning, diverse VHH sequences for each FMDV serotypes were observed (data not shown), while fifth and sixth rounds of panning were required to generate less diverse sequences more specific to capsid proteins of FMDV serotypes (Table 1). In the case of serotypes O and A, the CDR1 comprised seven amino acids in all the clones sequenced. Further, serotype O clones showed no variations in CDR1. But in serotype Asia1, 60% of the clones had seven amino acids length CDR1 and in 40% of the clone it was found to be ten amino acids. The CDR2 of serotype O and A comprised eight amino acids and it varied from 7 to 8 amino acids in serotype Asia1. Similarly, CDR3 consists of 17 amino acids in serotype O, 15 and 20 amino acids in serotype A, and 15 and 18 amino acids in serotype Asia1. It is to be noted that the average length of CDR3 in heavy-chain antibody is 16–18 amino acids. The CDR3 is considered to be the main contributor of antigen binding. It is also known that a longer loop length increases the paratope repertoire.

The hallmark substitutions established in the VHHs compared to the conventional VH at position 37 (F/Y), 44 (E), 45 (R/C), and 47 (G) in FR2 (7) are found to be F/V, E/D, R/H, and G/A, respectively, in the FMDV-specific clones. These residues in conventional VHHs form a hydrophobic surface association with VL and normally changed to hydrophilic residues in VHHs, such changes are believed to contribute to the

**Table 1.** The amino acid sequence of CDRs of serotypes O, A, and Asia1 VHH binders isolated after 6th round of panning.

FMDV	CDR1	CDR2	CDR3
Serotype O	STANIYN	QSISGALN	AARRGWAPSL SAYAYNY
Serotype A	NTYRRYC	NSAEGSTD	ALDGELSFAECRVGTTNFDY
	RPIGNFY	NTEGDGATY	ATGRSLFNSGWSRY
Serotype Asia1	DTFSNYC	KDGSATY	TFGIGSWCEFSYDY
	DAASTASTYC	SRGGGATY	AAGPLVSSCDYRYRAYTH

better folding and the solubility behavior of VHH. The characteristic serine residue at position 11 in FR1 was found conserved in all the sequences analyzed in the study. This substitution is considered as an adaptation to accommodate the absence of CH1 domain in camel VHH. The cysteine residue in FR1 at position 22 and FR3 at a variable position that form the characteristic disulfide bond was found fully conserved in all the sequences analyzed. The disulfide bonds between these cysteines that cross-link the antigen binding loops are believed to have a role in increasing the paratope repertoire (8).

### Expression of VHH in prokaryotic system

Expression of VHH rescued from the library was optimized in prokaryotic system using pET32 expression system. The constructs VHH-pET32 transformed in RosettaGami(DE3)PlacI for optimum yield of soluble VHH proteins on induction. Clear band was observed at 35 kDa that includes 15 kDa VHH tagged with TRX (Fig. 2a). The His-Trx-fused VHH could readily be purified using metal affinity chromatography method and was confirmed by Western blotting using anti-Histidine monoclonal antibodies (Fig. 2b).

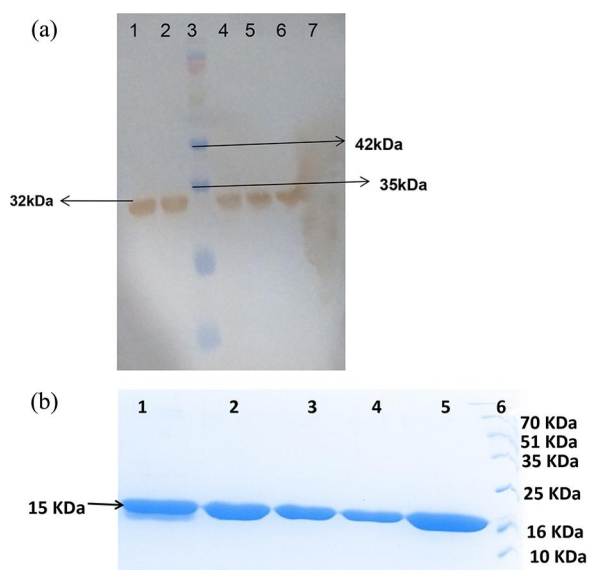


**Figure 2.** (a) Western blot and SDS-PAGE analysis of recombinant VHHs. Recombinant VHHs in pET 32 confirmed by western blot. Lane 3: puregene-prestained protein ladder. Lane 1, 2: serotype O VHHs, lane 4: serotype A VHHs, lanes 5 and 6: serotype Asia1 VHHs (expected size of 32 kDa). Lane 7: uninduced *Escherichia coli* RosettaGami DE3pLacl, and (b) SDS-PAGE after Ni-NTA purification where 15 kDa recombinant VHH is appreciated. Lanes 1 and 2: first flow-through of IMAC for K233, lane 3: first flow-through of IMAC for M101, lanes 4 and 5: first flow-through of M99 (expected size of 15 kDa). Lane 6: unstained protein ladder (Thermoscientific, USA).

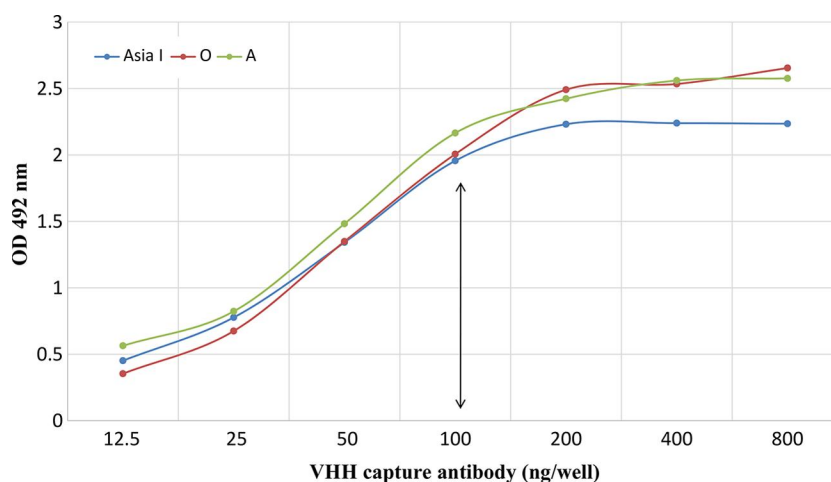


**Figure 3.** Optimization of recombinant VHH protein directed against FMD virus serotypes O, A, and Asia 1 for coating which was fixed at 100 ng/well concentration where the OD<sub>492</sub> lied between 2.0 and 2.3.

The expression tag hinders refolding under oxidizing environment of recombinant scFv antibody, whereas VHH has been demonstrated to retain its three-dimensional structure and biological activity due to single chain even after expression in the cytoplasm of *E. coli* cells (1,9).

#### Utilization of VHH as coating antibody

The cross-reactivity check followed by optimum concentration of VHHs to be used for coating was determined by checkerboard titration. The result was plotted graphically to estimate the quantity of proteins required for coating. Figure 3 depicts the cutoff point which was fixed at 100 ng/well for all three serotypes (serotype O, A, and Asia1). Further for the use of VHHs in LPB-ELISA, few minor changes were made in the existing protocol. The blocking buffer used was modulated a bit consisting of lactalbumin hydrolysate 3%, newborn calf serum 5%, and healthy camel serum 5% in PBST. A serial twofold dilutions of test serum are mixed with equal volume of a preoptimized constant dose of viral inactivated antigens in a liquid medium and allowed to react overnight at 4°C (6). Next day, the antigens, which are not completely blocked by the antibodies in the test serum, are trapped in the wells of the ELISA plates by the precoated type-specific VHHs. Antigen, negative and background controls are added containing antigen with PBS, antigen with healthy serum and blocking buffer, respectively. Subsequently, the presence of antigen is traced by adding pretitrated type-specific guinea pig serum and anti-guinea pig-HRPO conjugate. The dilution of guinea pig serum was optimized at 1:6000 for serotypes O and A, and 1:3000 for serotype Asia1. The anti-guinea

pig conjugate was used at dilution 1:2000. The plates were developed using substrate (OPD + H<sub>2</sub>O<sub>2</sub>) and the reaction was stopped after 15 min with 1 M H<sub>2</sub>SO<sub>4</sub> and measured in terms of optical density (OD) at 492 nm wavelength with reference to 620 nm.

Recombinant VHHs developed in this study can suffice the need of coating antibody without compromising the specificity and sensitivity of the test. To compare the performance of VHH-based LPB-ELISA and routine LPB-ELISA, 1023 serum samples obtained post outbreak were tested in both. A correlation was drawn taking the OD<sub>492</sub> values into consideration. Pearson correlation coefficient was high for serotype A (0.91) followed by serotype O (0.86) followed by serotype Asia 1 (0.82). Spearman's rank coefficient further depicted that the correlation was higher for serotype A (0.93) followed by serotype Asia 1 (0.92) followed by serotype O (0.90).

In conclusion, the developed LPB-ELISA using bacterially expressed anti-FMDV-VHHs have high correlation with that of standard LPB-ELISA. Though these recombinant VHHs have potential application in ELISA, epitope characterization of VHHs is essential to explore its use fully as a capture antibody in place of rabbit coating antibody. Study requires further validation by testing more number of serum samples. The study also showed that recombinant VHH production will help in increasing batch uniformity and decrease in the cost of sample testing (10). The biophysical characteristics make them appealing about being used in affordable and user-friendly diagnostic system (i.e., paper-based dipstick assay or filtration device). Ultimately, this study paves the way for the development of such paper-based devices which could demonstrate the practicality of an instrument-independent

method for visual detection of FMDV under various circumstances on-site.

## Acknowledgments

The authors express their gratitude to Professor Serge Muyldermans, Department of Molecular and Cellular Interactions, Vrije University Brussels, Belgium for his generous gift of vectors for construction of phage display library of single-domain antibodies. Authors wish to thank Dr Kashi Nath and workers from NRC on Camel, Bikaner for their kind assistance.

## Funding

ICAR and DST provided financial support for this work.

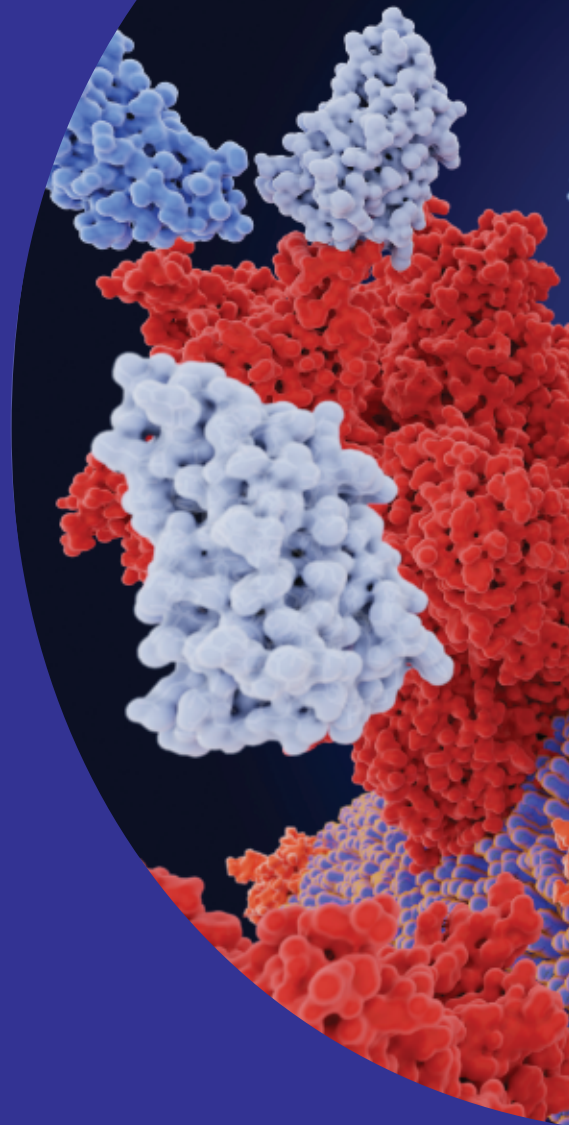
## ORCID

Lipsa Dash  <http://orcid.org/0000-0003-0775-5249>

## References

1. Muyldermans S. Nanobodies: natural single domain antibodies. *Annu Rev Biochem.* 2013;82:17.1–17.23.
2. Holliger P, Hudson PJ. Engineered antibody fragments and the rise of single domains. *Nat Biotechnol.* 2005;23:1126–36.
3. Ghassabeh GH, Saerens D, Muyldermans S. Isolation of antigen-specific nanobodies. *Antibody Eng.* 2010;2:251–66.
4. Vincke C, Gutiérrez C, Wernery U. Generation of single domain antibody fragments derived from camelids and generation of manifold constructs. *Methods Mol Biol.* 2012;9(7):145–76.
5. Pardon E, Laeremans T, Triest S. A general protocol for the generation of nanobodies for structural biology. *Nat Proto.* 2014;9:674–93.
6. Ranabijuli S, Mohapatra JK, Pandey LK. Serological evidence of foot-and-mouth disease virus infection in randomly surveyed goat population of Orissa, India. *Transbound Emerg Dis.* 2010;57:448–54.
7. Vu KB, Ghahroudi MA, Wyns L, Muyldermans S. Comparison of llama VH sequences from conventional and heavy chain antibodies. *Mol Immunol.* 1997;34:1121–31.
8. Desmyter A, Transue TR, Ghahroudi MA. Crystal structure of a camel single-domain VH antibody fragment in complex with lysozyme. *Nat Struct Mol Biol.* 1996;3:803–11.
9. Harmsen MM, Ruuls RC, Nijman IJ. Llama heavy-chain V regions consist of at least four distinct subfamilies revealing novel sequence features. *Mol Immunol.* 2000;37:579–90.
10. Marco AD. Biotechnological applications of recombinant single-domain antibody fragments. *Microb Cell Fact.* 2011;10:44.

**VHH Antibodies:  
Novel Engineering  
Strategies Beget  
Diverse Applications**



## Structural and biochemical properties of VHH antibodies

VHH antibodies, also known as single domain antibodies (sdAb) or heavy-chain antibodies (hcAb), are a monomeric variable antibody domain. The variable domains have a molecular weight of approximately 15kDa (about 10% that of conventional antibodies) and in nature are unique to camelids, including llamas and alpacas. VHH antibodies are found in the IgG2 and IgG3 subtypes which evolved without a CH1 domain and consist of a VH binding domain, extended hinge, and CH2 and CH3 domains (Figure 1). Recently, the advantages of VHH have become apparent in research, diagnostic, and therapeutic applications.

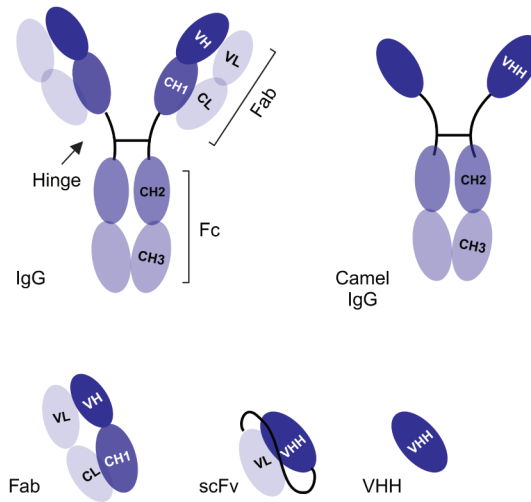


*Figure 1. Comparison of canonical IgG molecules, hcAb camelid IgG molecules, common Fv formats Fab and scFv, and the monomeric VHH domain.*

VHH antibodies exhibit unique characteristics in terms of framework and complementarity-determining regions (CDRs). The three complementarity determining regions (CDR1, CDR2 and CDR3) form the antigen-binding paratope. CDR1 and CDR2 have canonical structures and are found in the variable (V) region. CDR3, which has a non-canonical conformation, includes some of the V region, all of the diversity (D, heavy chain only) and joining (J) regions, and a piece of the constant (C) regions. While VHH domains lack VH-VL combinatorial diversity, the hcAb fragments have a longer CDR3 than either human or mouse VH antibodies and show lower conservation in the hypervariable regions. Compared with conventional camelid VH, llama VHHs differ by four amino acids in the FR2; positions (37, 44, 45, and 47). In the conventional VHs, these FR2 amino acids were conserved during evolution and are involved in forming the hydrophobic interface with the VL.

The CDR1 and CDR2 regions also show increased variability. Germline VHH antibodies have a conserved Cys22 and Cys92 disulfide bridge in all Ig domains, which provides stability, induces canonical Ig-like folding, and induces constraints in the orientation of the relationship between CDR1 and CDR3 regions. Combined, this allows VHH domains to evolve several novel binding modes to antigens that may be inaccessible to VH-VL binding. A common and high-value binding conformation would allow for CDR3 of the VHH to protrude beyond the typical interface and binds to clefts or grooves on a protein; this unique binding mode is particularly valuable in inhibition of enzymes or membrane-bound sites.

The hydrophilic nature of the VHH framework, in contrast to the hydrophobic VH framework, reduces the inclination for VH-VL mispairing in bispecific constructs. This characteristic causes the CDR3 of VHH antibodies to fold over onto the hydrophilic region, increasing stability.

## Methods of VHH library construction

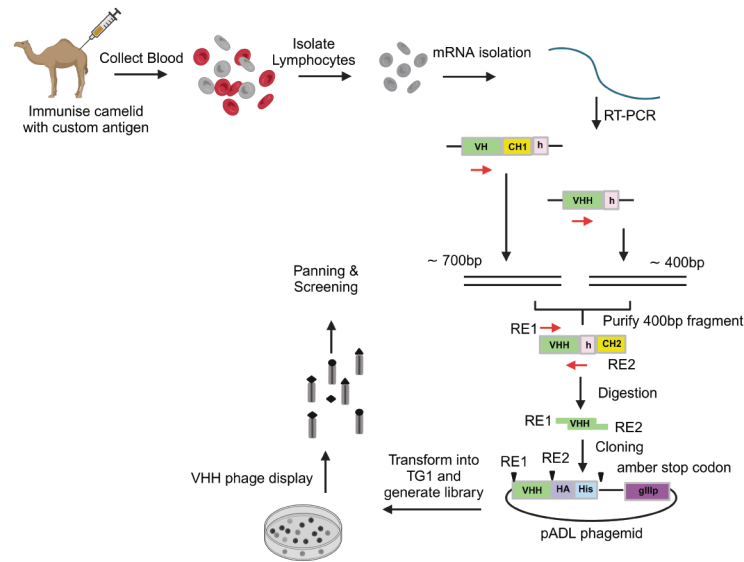


Figure 2. Overview of the Abcore immune library workflow, from injection and isolation to phage display library.

## Immunized VHH Library Construction and Panning

Immunization allows for endogenous affinity maturation processes to take place within the animal. Typical antigen is protein-based with the addition of adjuvant, but nanoparticles, liposomes, VLPs, whole cells, or genetic material has also generated robust immune responses in camelids. The process of constructing and panning immunized VHH libraries involves RNA isolation and cDNA amplification of llama peripheral blood mononuclear cells (PBMCs).

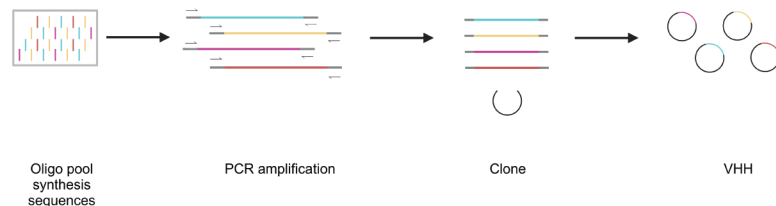


Figure 3. DNA library cloning. Many unique sequences are represented in one pool.

PCR amplification of the cDNA allows for isolation of the VHH band; due to sequence homology, the VH band and CH1 region are also amplified, but a purification step allows VHH product to be isolated (Figure 2). Additional PCR amplification steps depend on the vector being used, such as inserting the VHH library into yeast-displayed or phage-displayed fusions. Briefly, a molecular target is fixed to plates. Most commonly, protein is adsorbed onto polystyrene or biotinylated protein is bound to streptavidin-coated beads. Phage pools are added to the plates, and then unbound and weakly-binding phage are washed away. The remaining phage are eluted and amplified in bacteria, and the entire process is repeated multiple times to enrich for higher-affinity binding sequences (Figure 4).

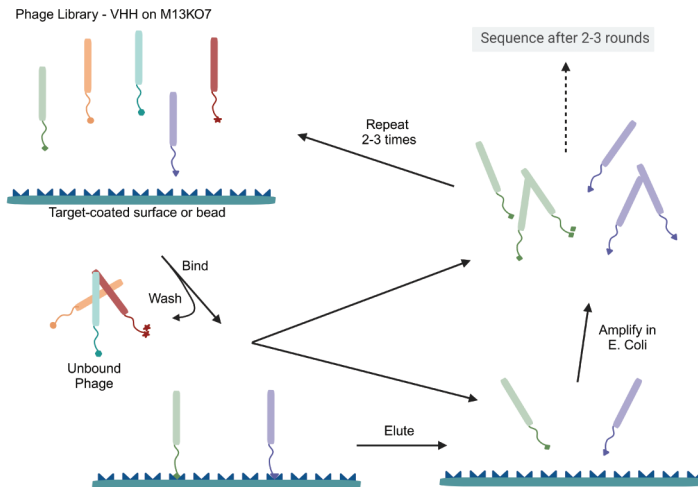


Figure 4. The phage display panning process.

## Synthetic VHH Libraries

Recent advancements have led to the development of high-quality commercial synthetic libraries for naïve humanized sdAbs. Advantages of synthetic libraries include diversity control in CDR regions, such as partially-degenerate codons, and the ability to tie in computational prediction methods with the diversification process, such as PyRosetta or AlphaFold pipelines. Synthetic libraries have difficulty sampling different lengths in CDR3, which is a major contributor to the diversity of binding mode in VHH interaction. Synthetic library sizes are determined in the design phase and typically range in diversity from 1E7 to 1E10 unique members.

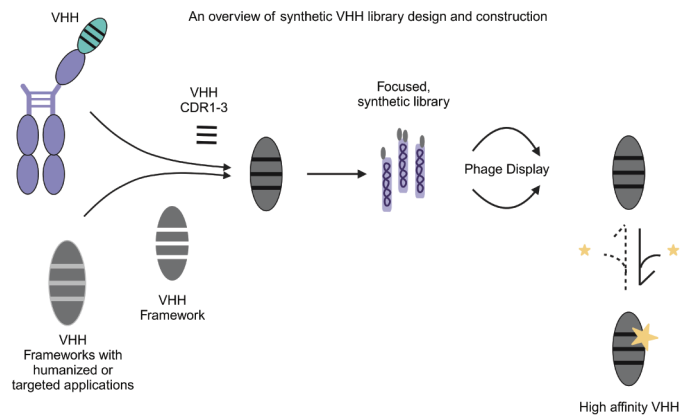


Figure 5. Synthetic VHH library design and construction.

## Considerations for selecting VHH over conventional antibodies

### Advantages of VHH Antibodies

1. **Smaller size:** The smaller size of VHH antibodies allows better access to antigen epitopes that may otherwise be inaccessible to larger antibodies. The smaller molecular weight of VHH antibodies changes several biophysical characteristics related to tissue perfusion and membrane permeability. Limited evidence also exists for an adsorptive endocytosis allowing for cell penetration and the potential to cross the blood-brain barrier.
2. **Thermostability and pH stability:** Compared with conventional antibodies where the paratopic interface between VL and VH is stabilized by hydrophobic residues in the FR2, hcAbs have evolved hydrophilic residues that are often charged in llama VHHs. VHH domains have less complex folding patterns than conventional antibodies, and

some VHH clones recover markedly better from denaturing conditions or heat shock than IgG molecules.

3. **Simplified workflow:** VHH antibodies simplify the discovery workflow as they do not require any crossed or paired workflows in cloning, expression, or assay projects. This single-domain advantage extends to functionalization workflows such as labeling and conjugation.
4. **Modulation of binding valency:** VHH antibodies can be engineered for a non-canonical binding valency depending on the desired functionality, such as activation, clustering, blocking, and specificity to multiple targets. Bivalent and tetravalent technologies exist as well as bispecific and trispecific recognition motifs. These technologies have emerging roles in therapeutics, synthetic biology, and diagnostic technologies.

### Disadvantages and Limitations of VHH Antibodies

1. **Requirement for llamas or alpacas:** Generating immunized libraries of VHH antibodies requires the housing and care of llamas or alpacas, leading to higher costs and space requirements compared to mouse models.
2. **Small interface size:** Due to the single-domain nature that imparts so many unique advantages, VHH antibodies exhibit lower affinity in binding to small antigens and peptides. This is most frequently due to a lower total buried surface area in the complex and may be addressed by engineering valency or affinity maturation techniques.
3. **Possible anti-drug antibody (ADA) effects:** Even with humanized VHH antibodies, the CDR3 loops themselves contribute more to immunogenicity than the innate framework residues, leading to potential ADA effects.
4. **Short serum half-life and rapid clearance:** VHH antibodies have a shorter serum half-life and are rapidly cleared. This limitation can be overcome through half-life extension modifications. In therapeutic contexts, however, this is less commonly an issue due to the fusion of VHH domains to a larger domain to trigger recognition such as an Fc domain.
5. **Structural integrity and stability:** Due to the limited total size, VHH antibodies have a maximum tolerance for manipulation in some binding modes. The smaller domain limits the number of first- and second-shell residues that may be engineered for improvements in affinity or specificity campaigns.

## Conclusion

The unique features of VHHs, including that they are: small; soluble; high affinity; thermostable; and have high expression yields in multiple systems, make them the ideal tool for a variety of applications including research, immunotherapy, diagnostics, in vivo imaging of tumors, and synthetic biology.

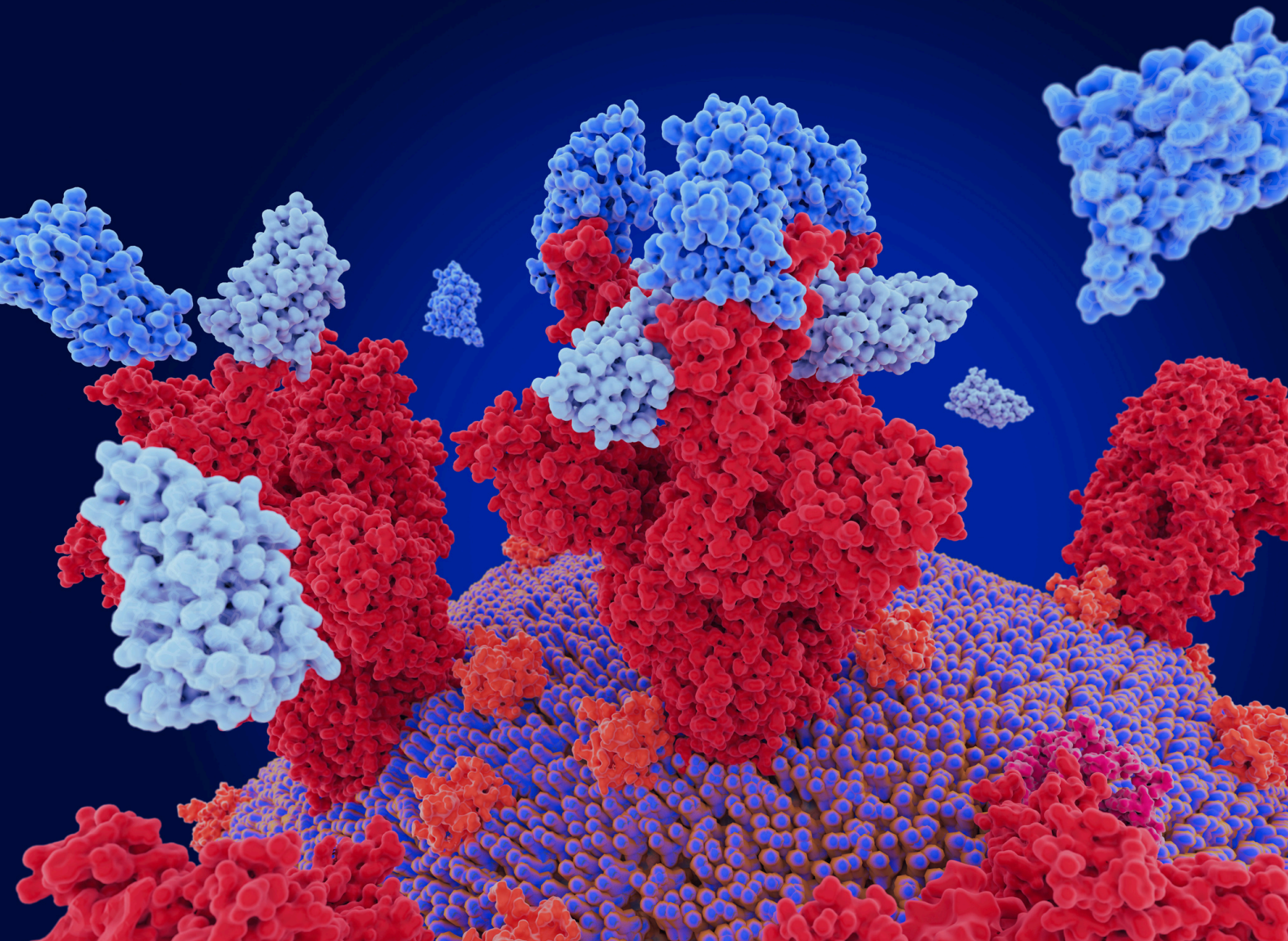
## About Abcore

Abcore is an industry leader in VHH discovery and custom antibody production located in sunny Southern California, USA. Abcore has developed a complete single-domain antibody platform based on antibody discovery via phage display and has made a variety of naïve and immunized phage display libraries that can be used for animal-free antibody discovery. Abcore offers a breadth of services across custom polyclonal, monoclonal, recombinant, and single-domain antibody production and is the largest camelid facility in the United States. As an established CRO, Abcore has worked with some of the world's largest biotechnology and pharmaceutical companies.



A FORTIS LIFE SCIENCES COMPANY





# Contact us

## Editorial Department

Senior Editor

Tristan Free

[Tristan.Free@tandf.co.uk](mailto:Tristan.Free@tandf.co.uk)

## Business Development and Support

Commercial Director

Evelina Rubio Hakansson

[Evelina.RubioHakansson@tandf.co.uk](mailto:Evelina.RubioHakansson@tandf.co.uk)

This supplement is brought to you by *BioTechniques* in association with



A FORTIS LIFE SCIENCES COMPANY